Reviewer comments in gray italics, my answer in black and the changes in the text in "…" and bold

Answer to referee 1

The authors have partly addressed my previous comments. However, two important points were eluded.

First, the authors acknowledge that there is an ***artifact in the interpolation scheme*** *that led to strange CO2 patterns in the North Sea, and an artificial difference between the west and the east side of the North Sea in particular in the SBNS that has been shown in the past as relatively homogeneous. They acknowledge that "These lines are a remnant of the open ocean pCO2 maps, which were used as a driver in the MLR (in this case Rödenbeck, 4x5˚ resolution)." However, they did little to try to correct this by adjusting/modifying the interpolation scheme. I do not see the added value of interpolating data and using fancy MRL approaches in an area where the data coverage is already very dense, to provide in the end clearly biased maps that the authors did not bother to try to correct.*

We regret that we have missed to address all the previously raised concerns by the referee. It was certainly not our intention to elude the important points raised. While we do understand and agree (hence our acknowledgement in the text) with the referee's argument that the coarse resolution nature of the open ocean driver data (namely the Rödenbeck 4x5 degree pCO2 field) and the resulting "patchy" pCO2 reconstruction appears too heterogenous in contrast to other studies. The referee therefore suggests correcting our approach in order to improve performance, however there are some noteworthy complications that prevent us from doing so.

Firstly, the construction of the input data for our MLR is out of our hand. While we would benefit from a finer resolved Mixed Layer interpolation scheme by Rödenbeck et al, (and equally finer resolved physical proxies such as temperature and salinity, etc) this is not feasible considering the built-up of the method. That said, Rödenbeck et al have now created a finer resolved version of their scheme (with 2.5˚ x 2˚ resolution), however, even with this finer resolved version we still see this spatial gradient. Other products with higher resolution that extend to the coast and may serve as an alternative for the future are currently in review (see also Laruelle et al and the product of Landschützer et al 2020 and discussion below), but none of these alternative products offers a resolution attempted in our study. Our primary intention is to make use of the coarse resolution existing pCO2 estimates to provide novel and fine-resolved coastal estimates, but not to improve the existing estimates. That said, we believe this still is valuable information.

Secondly, we believe it behooves us well to highlight shortcomings of our approach, even when they are outside our ability to change. That said, we agree that this deserves a more detailed discussion than previously provided.

Thirdly, we agree with the argument by the referee that direct measurements do not show these gradients as strongly and are therefore more reliable. Nevertheless, for many applications, such as model evaluation or the investigation of regional trends a high-resolution gap-filled pCO2 product is required, desired or even inevitable. In addition, the amount of

available data is not such that they can be mapped with confidence every single year. We have first-hand experience, and gaps due to instrumental failure and funding issues, do occur. Here we offer a first, though not bias-free, estimate that aims to be applied to all coastal regions of the western Nordic Seas, discussing its shortcomings and offer ways forward to improve it in the future. One way forward would be to improve the resolution of the open ocean pCO2 product. A second possible way forward would be to apply different drivers, as we potentially do not need pCO2 as a driver for data rich regions. Illustrating and discussing ways forward is certainly something we have missed in our previous manuscript and our first response to the referee's concerns, however, working out the technical aspects is, as we still believe, beyond the scope of this study. In this study we focus on the best and most robust scheme for all regions combined.

Therefore, considering the point raised by the referee and our answers above, we have extended the discussion and added the following:

In the Results (p 10, l 11 – p 12, l 6):

"We notice that the gradients that exist between the grid cells in the Rödenbeck map, are still visible in our maps in some regions, for example the sharp gradient in the southern North Sea in February, or the east-west and north-south gradients in the entire North Sea in August. Such gradients are also evident in directly mapped pCO_2 data (Kitidis et al. 2009), however, here they are more strongly meridional and latitudinal in their extent. As such, while these gradients do reflect actual features of the pCO_2 distribution in the North Sea, their specific shape here, are also a consequence of the influence of the Rödenbeck maps on our estimates; from the use of these maps as a driver in the MLR and their importance in improving the statistical performance vs the MLR that did not use these values as a driver (MLR 1 vs MLR 3, Table 5). Also, they do reflect the uncertainty of - and our level of confidence in - the estimated pCO_2 values; being approximately similar to or slightly larger than the RMSE of MLR 1 (Table 5). Any smoothing would be completely artificial, and, while being more visually pleasing, would not better reflect the truth in any meaningfully quantifiable extent. We have therefore chosen to leave them untouched. These gradients are therefore also visible in subsequent pH and trend maps."

In the Discussion (p 14, l 9 – l 7):

"One clear drawback of the here presented MLR 1 is the clearly visible grid-pattern of the open ocean pCO_2 product that was used as input data with its grid size of 5˚ x 4˚. This artifact implies sharper gradients in fCO_2 than can be found in observations. There are two ways how one could get rid of this artifact in a future release. A finer resolution of the used open ocean maps will lead to a better representation of the actual gradients in our mapped product. Rödenbeck et al. just released a newer, finer resolution of their open ocean product that we intend to use in a future version of this data product. Additionally, running the MLR without an open ocean pCO_2 product can provide a coastal pCO_2 product without this artifact (given that all other driving parameters, such as temperature or mixed layer depth, also are available in the required resolution). While in principle it is preferential to have coastal maps that are independent of the open ocean

products, MLR 3, which is running without open ocean pCO_2 as driver, did not reach the same accuracy as MLR 1. New and better input fields or a different regression method could help improving the independent coastal maps in the future."

Second, the authors acknowledge that the pCO2 shows a shift in the spring bloom timing. This is a really interesting result that would strongly contribute to the future impact of this work. So I do not understand that the authors did not include this in the paper, I do not see how this could be "outside the scope of this work" as replied.

Again, it was certainly not our intention to elude the important points raised and agree that this observation should be included and explored to a larger extent in the discussion. We do believe, however, it is "out of scope" for us to quantify the reason why this shift has happened, as this would entail detailed examination of the atmospheric, oceanic and ecosystem conditions that can bring about such a change. We also note, that the monthly resolution of our maps somewhat restricts abilities to detect changes in the timing of the onset of the spring bloom, as such changes may be a matter of days to weeks. That being said we do see a significant shift the bloom timing in the western North Sea between the first and the second half of our time series. We added a panel showing the average pCO2 seasonalities in the northwestern North Sea from 1998 to 2007 and 2007 to 2016. We also added extended discussion and added an additional panel to Figure 10.

(p 20, l 18 – p 21, l 6)

"Figure 10a shows the annual trends in fCO_2 in each month in the four regions considered. Particularly in the North Sea and Baltic, very low fCO_2 trends are observed in February – May, suggesting that changing timing of the spring bloom might be important here. Investigating the seasonal fCO_2 in more detail (Figure 10b), revealed an earlier and deeper fCO_2 drawdown in the second decade of our analysis (2007-2016) than in the first (1998-2007) in the northeastern North Sea (58 – 60˚N, 3 -8˚E). This strongly suggest that an earlier and stronger spring bloom is lowering the annual pCO_2 growth rates in this region, which is among the ones with the smallest fCO_2 trends (X μatm yr^{-1}, Fig. 9). In the other regions, no such changes could be established with confidence. Future investigations should aim at generating fCO_2 maps with higher temporal resolution, as changes in the timing of the spring bloom might be a matter of days or weeks, which would not be fully resolved by the monthly maps presented here."

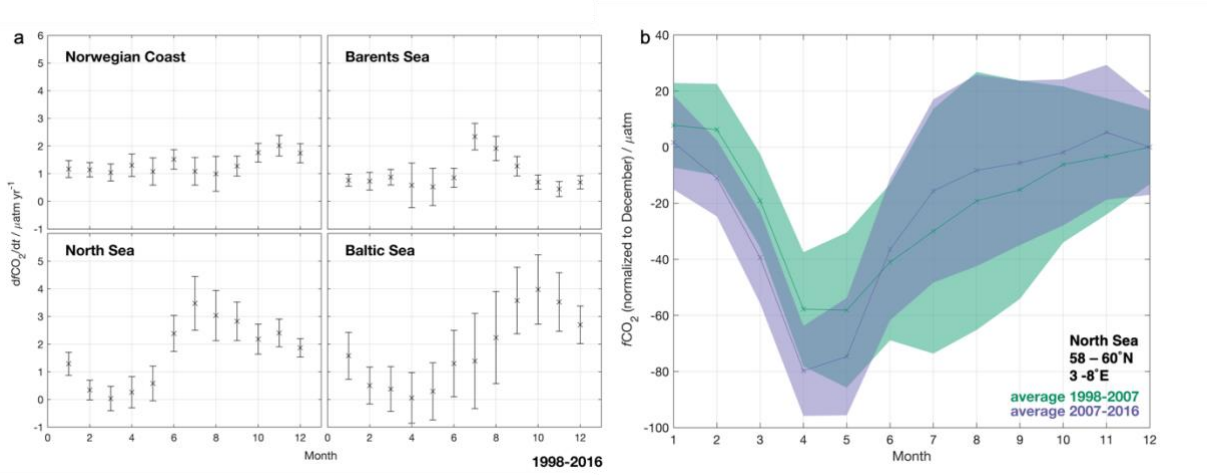

Figure 10: (a)The trend in surface ocean fCO_2 estimated resolved per month (1998 to 2016). (b) The average seasonality in fCO_2 for the periods 1998-2007 (green) and 2007-2016 (purple) in the northeastern North Sea (58 – 60˚N, 3 -8˚E), normalized to December. The standard deviation for each month is shown as shaded area.

Can the authors add to the discussion how their approach compares to the recent work of Landschützer et al. (2020) that seem to provide a consistent and uniform interpolation scheme for the open and coastal oceans.

At the time of initial submission, the study by Landschützer et al 2020 was not yet submitted and the submission of the 1st revision the study only existed as a pre-print (i.e. has not undergone peer review in its online form). To follow rigorous scientific standards, we try and avoid discussing grey literature. Fortunately, the study by Landschützer et al 2020 has now been accepted for publication. We understand the resemblance between these studies and the resulting need for clarification. There are several major differences between the study of Landschützer et al 2020 and this work:

Firstly, Landschützer et al 2020 do not provide a new estimate in our chosen study domain, but combines the open ocean estimate by Landschützer et al 2016 with the coastal ocean estimate by Laruelle et al 2017. Therefore, most regions that are both covered in our study and in the Landschützer et al 2020 estimate actually stem from Laruelle et al 2017, which we do discuss in our manuscript.

Secondly, Landschützer et al 2020 combine their estimates to provide a 0.25x0.25 degree climatology covering the global ocean. Here, we, on the one hand, provide a higher resolution local estimate, which on the other hand focuses on longer term signals rather than seasonal variations.

To acknowledge the existence of this climatology, and its potential to further improve our local high-resolution approach, we added to the text:

(p 2, l 22 – l 24)

“A global climatology covering both open ocean and coastal regions was recently

performed by combining this product with the open ocean product of Landschützer et al (2016) (Landschützer et al.,2020).”

Refs

Landschützer, P., Laruelle, G. G., Roobaert, A., and Regnier, P.: A uniform pCO2 climatology combining open and coastal oceans, Earth Syst. Sci. Data Discuss., https://doi.org/10.5194/essd-2020-90, in review, 2020.

Reviewer comments in gray italics, my answer in black and the changes in the text in "…" and bold

Answer to referee 2

Many of the issues raised in the first review have been well addressed but the authors have argued that they do not wish to address others.

The unwillingness to publish the actual MLR equation used remains a concern. The given reason is "We recommend strongly to develop a specific fit for any new application." What if the new application is to directly compare the result here with another MLR - to compare the directions and relative importance of the variables driving the fit - either developed for the same region with newer data or for a different region? Not showing the different terms also hinders assessment of whether the fit makes sense, whether terms with well-known relationships with pCO2 (e.g. temperature) are driving it in the expected direction, whether the relationships are meaningful and linked to underlying processes (and therefore probably more reliable for predicting beyond the input dataset) or simply spurious correlations for the specific training data used. Finally, keeping something so critical to the study as a secret "black box" seems to contradict the open access principles of this journal.

We regret that we have missed to address all the important points by raised the referee during the first revision. It was certainly not our intention to hide the MLR coefficients, but our first intuition was, that the equations are strongly optimized for the chosen study domain, hence we wanted to avoid the impression we have created a generalized MLR model (that may be applied to other regions as well). In spite of our initial intention we may indeed have missed the opportunity to be transparent and instead presented a black box. That being said, we think that the use of the MLR coefficients for interpretation is limited because (a) many drivers (e.g. chlorophyll) serve as proxies for higher order processes, (b) many drivers have manifold and sometimes opposite influence on the carbonate system (e.g. temperature effects both the gas solubility as well as the Schmidt number but can act as a proxy for upwelled cold deep water) which makes a direct interpretation of the coefficients challenging. However, we as mentioned above, we certainly don't want to hide the equations, hence we now added the equations of the MLR to the supplementary.

We added the following to the manuscript:

(p 9, l 19 – l 20)

«The coefficients for MLR 1, MLR 2 and MLR 3 are provided in the supplement. «

The comparison between previous results in Table 1 vs the significance plot in Figure 9 has not been addressed. The authors may of course decide that discussing the actual drivers (e.g. NAO) of interannual variability is beyond the scope of this study. But even ignoring

the drivers, the point remains that the new results here show that trends determined over the short periods that were the basis of previous studies are not significant. As things stand, a new result that implicitly casts doubt on earlier work is being presented here without comment.

We are sorry that we did not address the concern of incompletely discussing our results in a satisfactory way. In the following we want to give a detailed answer to both discussion points raised by the referee.
Regarding the actual drivers of the shown interannual variability, we do think that this topic easily can get very extensive and is better addressed in a separate manuscript, particularly in light of multiple climate modes dominating on various timescales (see e.g. Landschützer et al 2019, GRL, "Detecting regional modes of variability in observation-based surface ocean pCO_2) and potential teleconnections (see, e.g. Steinman, B. A., M. E. Mann, and S. K. Miller (2015), Atlantic and Pacific multidecadal oscillations and Northern Hemisphere temperatures, Science, 347, 988, doi:10.1126/science.1257856). That being said, we did test if the NAO, i.e. the climate mode previously identified as the dominant mode of variability in these regions, can explain at least some of the interannual variability that we observe. As we did not find any significant correlation over the entire study area, we decided not to concentrate further on this. However, the referee is correct in pointing out that also not finding a significant correlation is worth mentioning.

We completely agree with the referee that the non-significant pCO_2 trends for time ranges of less than 10 years is an important finding and needs to be stated. We deeply regret that we missed addressing this in the original manuscript.

To amend these to shortcomings we added the following two paragraphs to the manuscript:

(p 24, l 23 – l 27)

«There is an ongoing discussion, how and to which extend the dominant climate mode in the North Atlantic, the North Atlantic Oscillation (NAO) is driving the variability in the CO_2 fluxes (Tjiputra et al. 2011, Salt et al, 2013, Watson et al, 2009). Even though some features in the time series seem coincident with very extreme states of the NAO, such as a very large disequilibrium along the Norwegian Coast in 2010, we could not find any significant correlation between the CO_2 fluxes and the NAO index.»

(p 18, l 26 – l 30)

«Generally, only few regressions over time ranges of less than 10 years turned out to be significant. This is an important finding when comparing the trends determined from our maps with the trends reported in literature, of which many were covering periods shorter than 10 years (Table 1). In order to compare the general patterns of fCO_2 determined from our maps with those directly determined from observations over a similar time range, we estimated the fCO_2 trends also from the SOCAT v5 observations that were used to produce the MLR (Table 6).»

*The issue regarding the **northern Baltic Sea** containing only a single month of data was acknowledged in the author responses but it would be better to discuss this briefly in the manuscript itself. Looking back to the map on Figure 9 it's interesting to see that this region does not have black dots to indicate non-significant trends. The method therefore claims to identify a significant long-term trend for a region containing only one month from one year of training data. This makes me wonder whether significance is being assessed in a suitable way.*

We regret that we gave the referee the impression of not handling the uncertainties in an acceptable way. Figure 9 only shows the significance of the trend regression. This is independent of how much data there is to produce the MLR in the first place. We do state clearly that especially the data in the northern Baltic Sea have to be handled with care. That being said, we do understand that not marking these as questionable in Figure 9 may lead the reader to trust the trends in the Bay of Bothnia. We therefore removed this region from Figure 9.

(p 18, l 10 – l 12)

«We exclude the northern Baltic Sea from the trend map because we do not expect to have a robust trend estimate in that region as there are only very few data from that region in the regression. «

The northern European shelf as increasing net sink for CO_2

Meike Becker[1,2], Are Olsen[1,2], Peter Landschützer[3], Abdirhaman Omar[4,2], Gregor Rehder[5], Christian Rödenbeck[6], and Ingunn Skjelvan[4,2]

[1]Geophysical Institute, University of Bergen, Bergen, Norway
[2]Bjerknes Center for Climate Research, Bergen, Norway
[3]Max Planck Institute for Meteorology, Hamburg, Germany
[4]NORCE Norwegian Research Centre AS, Bergen, Norway
[5]Leibniz Institute for Baltic Sea Reasearch, Warnemünde, Germany
[6]Max Planck Institute for Biogeochemistry, Jena, Germany

Correspondence: Meike Becker (meike.becker@uib.no)

Abstract. We developed a simple method to refine existing open ocean maps and extending them towards different coastal seas. Using a multi linear regression we produced monthly maps of surface ocean fCO_2 in the northern European coastal seas (North Sea, Baltic Sea, Norwegian Coast and in the Barents Sea) covering a time period from 1998 to 2016. A comparison with gridded SOCAT v5 data revealed mean biases and standard deviations of ~~the residuals~~ $0\pm26\mu$atm in the North Sea, $0\pm16\mu$atm along the Norwegian Coast, $0\pm19\mu$atm in the Barents Sea, and $2\pm42\mu$atm in the Baltic Sea. We used these maps ~~as basis~~ to investigate trends in fCO_2, pH and air-sea CO_2 flux. The surface ocean fCO_2 trends are smaller than the atmospheric trend in most of the studied ~~region. Only~~ regions. The only exception to this is the western part of the North Sea~~is showing an increase in~~ , where sea surface fCO_2 ~~close to~~ increase by 2 μatm yr^{-1}, which is similar to the atmospheric trend. The Baltic Sea does not show a significant trend. Here, the variability was much larger than ~~possibly observable~~ the expected trends. Consistently, the pH trends were smaller than expected for an increase of fCO_2 in pace with the rise of atmospheric CO_2 levels. The calculated air-sea CO_2 fluxes revealed that most regions were net sinks for CO_2. Only the southern North Sea and the Baltic Sea emitted CO_2 to the atmosphere. Especially in the northern regions the sink strength increased during the studied period.

1 Introduction

For facing global challenges, such as predicting and tracking climate change, it is important to improve our understanding of the ocean carbon sink and its variability. Open oceans, especially those of the northern hemisphere, are relatively well understood and described in their large-scale variability (Gruber et al., 2019; Landschützer et al., 2018, 2019; Fay and McKinley, 2017). Reliable autonomous systems for measuring carbon dioxide partial pressure from commercial vessels were developed in the early 2000s (Pierrot et al., 2009) and have since been deployed on a large number of vessels (e.g. ~~(Bakker et al., 2016)~~ Bakker et al. (2016)). This has resulted in sufficient data to develop methods to interpolate the data and to describe large scale

air-sea CO_2 exchange and its variability (Landschützer et al., 2014, 2013; Rödenbeck et al., 2013; Jones et al., 2015). These methods ~~cover a~~ apply wide variety of approaches, such as linear ~~interpolations~~interpolation, machine learning, and model based estimates. By comparing the different results, it is possible to achieve a good estimate of the uncertainty associated with the respective methods ~~and to evaluate their performance relative to each other~~ (Rödenbeck et al., 2015).

Despite ~~coasts~~ coastal seas cover 7-10% of the world's oceans (Bourgeois et al., 2016), their contribution to the oceanic carbon sink is not yet fully constrained. Whether coastal ~~oceans~~ seas are a net sink or source for atmospheric CO_2 and how their role will change in a changing climate is still under debate (Bauer et al., 2013; Laruelle et al., 2010). Compared to the open ocean, longer time series and ~~a~~ higher spatial and temporal resolution of the observations are needed in order to capture all relevant coastal processes. ~~Circulation patterns such as small currents caused by the topography, or tidal cycles~~ Small scale circulation patterns governed by topographic features, thermal and haline stratification, or mixing through tidal cycles, upwelling or internal waves result in a need for more complex maps with a higher resolution ~~(Bricheno et al., 2014; Lima and Wethey, 2012~~ (Bricheno et al., 2014; Lima and Wethey, 2012; Blanton, 1991). These physical drivers are not the only reasons for ~~coasts~~ coastal seas being more complicated to understand. ~~Processes taking place in the sediments or respiration of sinking material do not directly affect the surface in the open ocean . In shallow coastal regions the water column can easily be mixed all the way to the bottom allowing for echange~~ Generally, coastal regions are more productive than open ocean regions due to better availability of nutrients (e.g. mixing at continental margins, river runoff). While deeper coastal regions are seasonally stratified, shallow regions are vertically mixed allowing for exchange between the benthic and ~~pelargic~~ pelagic parts of the ecosystem ~~(Griffiths et al., 2017).~~ (Griffiths et al., 2017; Wollast, 1998). Together with strong gradients of productivity this leads to spatial and temporal heterogeneity in surface CO_2 content.

The different maps developed for describing the open ocean surface pCO_2 (CO_2 partial pressure) dynamics and air-sea CO_2 fluxes are not directly ~~suitable for use~~ applicable in coastal regions. Many exclude data from ~~coastal regions~~ continental shelves completely while all of them have ~~a~~ too coarse spatial resolution ~~to properly resolve the coast with its small-scale variability~~ (typically between 1 and 5 °) to properly resolve coastal seas with their small-scale variability. A few studies ~~tried to describe~~ have described coastal carbon dynamics but most of them ~~had~~ have strong regional or temporal limitations. Table 1 shows an overview of studies with estimated pCO_2 trends over the northern European shelf while Table 2 presents available flux estimates. Laruelle et al. (2017) used a neural network approach to produce a global pCO_2 climatology ~~of coastal oceans~~for coastal seas, describing more distinct seasonal variability in the northern hemisphere than in the southern Pacific and Atlantic. ~~Few studies attempted to constrain coastal air-sea fluxes before~~A global climatology covering both open ocean and coastal regions was recently constructed by combining this product with the open ocean product of Landschützer et al. (2016) (Landschützer et al., 2020). Laruelle et al. (2018) published trend estimates in regions with ~~a~~ high data coverage based on winter data spanning up to 35 years~~finding~~. Their findings is that the pCO_2 rise in coastal regions ~~to lag behind~~ tend to lag the atmospheric rise in CO_2. However, few studies attempted to constrain coastal air-sea fluxes before. Kitidis et al. (2019) estimated fluxes between 0 and -15 mmol m^{-2} day^{-1} in the North Sea, depending on the season (more negative during summer than during winter) and the region (more negative fluxes in the norther North Sea compared to the south). For the Baltic Sea, Parard et al. (2016, 2017) used a neural network approach to produce surface ocean pCO_2 maps from 1998 to 2011

Table 1. Overview of trends in surface ocean CO_2 reported in the literature.

	Reference	Time range	$dpCO_2/dt$ /μatm yr^{-1}
North Sea	Thomas et al. (2007)	2001-2005, summer data normalized to 16°	7.9
North Sea	Salt et al. (2013)	2001-2005, summer data, normalized to 16°	6.5
North Sea	Salt et al. (2013)	2005-2008, summer data, normalized to 16°	1.33
Faeroe Banks	Fröb et al. (2019)	2004-2017, winter data (DJFM)	2.25 ± 0.20
North Sea, west	Omar et al. (2019)	2004-2017, winter data (DJ)	2.19 ± 0.55
North Sea, east	Omar et al. (2019)	2004-2017, winter data (DJF)	not significant
North Sea	Laruelle et al. (2018)	1988-2015	almost no trend
English channel	Laruelle et al. (2018)	1988-2015	slightly smaller than atmosphere
Baltic Sea	Wesslander et al. (2010)	1994-2008	larger than atmosphere
Baltic Sea	Schneider and Müller (2018)	2008-2015	4.6 - 6.1
Baltic Sea, west	Laruelle et al. (2018)	1988-2015	much smaller than atmosphere, slightly negative
Barents Sea	Yasunaka et al. (2018)	1997-2013	not significant
Barents Sea	Laruelle et al. (2018)	1988-2015	about the same as atmosphere
Atmosphere	global average	1997-2016	2.02 ppm yr^{-1}

and estimated an air-sea flux of 1.2 mmol m^{-2} day^{-1}. Yasunaka et al. (2018) estimated a flux of 8 - 12 mmol m^{-2} day^{-1} in the Barents Sea and along the Norwegian coast using a self-organizing map technique. Most of the other available studies on the trends in coastal pCO_2 are based on data from either summer or winter. Estimates based on summer-only data typically show large interannual variations (Thomas et al., 2007; Salt et al., 2013), which led to the conclusion that here the interannual variability masks the actual long term trend. The approach to use winter-only data (Fröb et al., 2019; Omar et al., 2019), on the other hand, is based on the assumption that during this season the influence of biological processes is negligible and therefore winter data can be used to establish a baseline trend. However, also using winter-only data has its drawbacks. In particular the choice of which months to include can cause biases and the optimal selection can differ from region to region.

In this study we present a new approach to develop monthly fCO_2 (CO_2 fugacity) maps based on already existing open ocean pCO_2 maps, in four example regions: North Sea, Baltic Sea, Norwegian Coast and the Barents Sea~~, with the aim to determine the air-sea CO_2 exchange in these regions and its decadal trends~~. A multi linear regression (MLR) was used ~~, fitting~~ to fit driver data against fCO_2 observations. Based on the resulting fCO_2 maps and a salinity-alkalinity correlation we also produced monthly maps of coastal pH. The performance of the produced maps was evaluated and the maps were then used to investigate trends in coastal fCO_2 and pH in the entire region from 1998 to 2016. Finally, we ~~calculated~~ used the fCO_2 maps to determine the air-sea CO_2 ~~fluxes and show their~~ exchange and its temporal and spatial patterns.

Table 2. Overview of air-sea CO_2 fluxes reported in the literature. Negative sign denotes flux from atmosphere to ocean.

	Reference	Time range	F / mmol m^{-2} day^{-1}
North Sea	Meyer et al. (2018)	2001/2002	-3.8
North Sea	Kitidis et al. (2019)	2015	0 - -15
Baltic Sea	Parard et al. (2017)	1998-2011	1.2
Norwegian Coast	Yasunaka et al. (2018)	1997-2013	-4 - -8
Barents Sea	Yasunaka et al. (2018)	1997-2013	-8 - -12

2 Method

2.1 Study area

This work focuses on ~~northern European coasts~~ the northern European continental shelf and marginal seas. As we want to show the performance of the MLR method we picked a number of regions with very different characteristics: the North Sea, the Baltic Sea, the Norwegian coast and the western Barents Sea (Figure 1). We decided to concentrate on these regions ~~specifically~~ because (1) the data coverage in these regions is fairly high and (2) the authors have strong knowledge on the specific regions. This is important in order to properly evaluate the maps and to assess whether or not the output is realistic. The ~~4~~ four regions were defined based on the COastal Segmentation and related CATchments (COSCAT) segmentation scheme (Laruelle et al., 2013). The threshold for defining a region as coastal sea was set to a depth limit of 500 m~~(Figure 1)~~. By using this definition, we produce an overlap to the open ocean maps, allowing our maps to be merged with the open ocean maps. Please note, that this study concentrates on the continental shelf area. The near coastal zones (e.g. intertidal zones) are not included due to the limited availability of driver data in these regions.

2.2 Data handling

The CO_2 data used in this study were extracted from SOCAT version 5 (Bakker et al., 2016). Their coverage is shown in Figure 2. A newer version of the SOCAT database (SOCATv2019) was used for validating the maps against independent data. An overview over the reanalysis products used as driver data is given in Table 3. We use as basic driver data sea surface temperature (SST), sea surface salinity (SSS), chlorophyll a concentration (Chl a), mixed layer depth (MLD), bathymetry (BAT), distance from shore (DIST), ice concentration (ICE) ~~,~~and the change in ice concentration from the month to month (prior to current). Chl a values during the dark winter season were set to 0. In addition to the reanalysis data, pCO_2 values from the closest coastal grid cell of the open ocean map ~~was~~ were used as a driver in our MLR. We ~~can neglect the~~ neglect the approximately 1 μatm difference between partial pressure (reported in the mapped products) and fugacity of CO_2 (~~about 1 μatm) at this place~~ reported in SOCAT) as it is much smaller than the accuracy of the data extracted from SOCAT v5 (2 to 10 μatm) and the uncertainty associated ~~to~~ with the open ocean maps. The open ocean pCO_2 values were extracted from two different products (Rödenbeck et al. (2014) (version oc_v1.5) and Landschützer et al. (2017, 2016) (version 2016)). Rödenbeck et al. (2014) is

based on a data-driven diagnostic model of mixed layer ocean biogeochemistry fitted against surface pCO_2 observations while Landschützer et al. (2016) ~~is based on~~ uses a two-step neural network (a feed-forward network coupled with self-organizing maps, FFN-SOM) trained with the pCO_2 observations. Please note that the Rödenbeck open ocean map ~~also~~ contains data in coastal grid boxes, while the Landschützer open ocean map is restricted to the open ocean regions~~south of 80°N~~. The MLR models based on these two are called MLR 1 (based on the coastal pCO_2 values from the Rödenbeck map) and MLR 2 (based on the the nearest open ocean pCO_2 values of the Landschützer map), respectively. To determine the extent to which the regressions benefit from the information in the open ocean maps, a third MLR, MLR 3, was determined. ~~This does not have~~ Here, we do not use any of the open ocean maps as driver, but ~~instead uses the year as proxy~~ to account for the annual rise in CO_2, year is included in the set of driver data.

For ~~producing~~ preparing the input data for the MLR, observations closest to each SOCAT fCO_2 data point ~~was assigned to the closest data point in space and time of each of the reanalysis~~ in time and space were extracted from the 3D fields with the driver data. This produces~~a matrix~~ , for each of the driver data, a vector as long as the SOCAT fCO_2 observations~~for each driver data~~. After this, the fCO_2 data as well as all extracted driver data were binned on a monthly 0.125°x0.125° grid covering ~~1998~~ 1997 to 2016. ~~This step ensures~~ These procedures ensure that the driver data have the same bias in space and time within each grid box as the fCO_2 data. If a grid box for example only contains fCO_2 observations from the first week of the month and the northwestern corner, we make sure, that also the gridded driver data only contains values from the first week and the northwestern corner of the grid box, and not an average over the entire month and grid box. This is mostly important for the chlorophyll driver data, which are available ~~in~~ at a very high resolution compared to the fCO_2 maps produced in this work. These driver data were used for ~~the MLR~~determining the MLRs.

For producing the final maps, a second set of the driver data was ~~produced~~prepared, in the following called field data. Here the driver data were directly regridded to a monthly 0.125°x0.125° grid, providing ~~the~~ full spatial and temporal coverage and a ~~homogene~~ homogeneous average in each grid box. The field data were used to produce the fCO_2 maps based on the equation derived ~~from the MLR~~ MLR equations.

2.3 Multi linear regression

The multi linear regression models were constructed by forward and backward stepwise regression using the driver data as predictor variables to model the fCO_2 observations. ~~During a stepwise regression in each step ,~~ In each step of this regression procedure, the model's tolerance to addition or exclusion of a variable is tested~~for being added or removed from the set of explanatory variables~~. This decision on whether to add or remove a term ~~was~~ is based on the p-value of the F-statistic with or without the term in question. The entrance tolerance was set to 0.05 and the exit tolerance to 0.1. The model includes constant, linear, and quadratic terms as well as products of linear terms. Equation 1 gives the basic equation, with $X_1 ... X_n$ being the driver data and $a_1 ... a_{nn}$ the regression coefficients.

$$y = a_0 + a_1 \cdot X_1 + ... + a_n \cdot X_n + a_{12} \cdot X_1 X_2 + ... + a_{mn} \cdot X_m X_n + a_{11} \cdot X_1^2 + ... + a_{nn} \cdot X_n^2 \quad (1)$$

Table 3. Products used as driver data in the MLR and the maps.

Product used	Resolution	Reference
Chl a for MLR	4km x 4km, 8 days	Global Ocean Chlorophyll (Copernicus-GlobColour) from Satellite Observations - Reprocessed
Chl a for maps	4km x 4km, monthly	Global Ocean Chlorophyll (Copernicus-GlobColour) from Satellite Observations - Reprocessed
MLD	12.5km x 12.5km, monthly	Arctic Ocean Physics Reanalysis
ICE	0.25°x0.25°, monthly	Cavalieri et al. (1996)
SST / SSS	0.25°x0.25°, weekly	Global Ocean Observation-based Products Global_Rep_Phy_001_021
BAT	2min x 2min	ETOPO2v2 Center (2006)
Rödenbeck pCO_2	5° x 4°, monthly	Rödenbeck et al. (2014)
Landschützer pCO_2	1° x 1°, monthly	Landschützer et al. (2017)

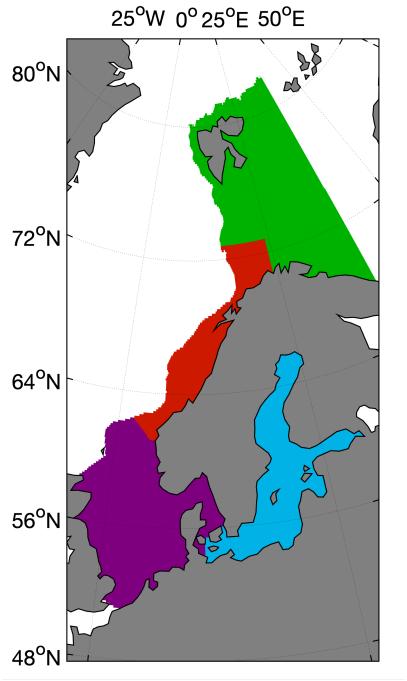

Figure 1. The study area and the location of the four different regions North Sea (purple), Norwegian Coast (red), Barents Sea (green) and Baltic Sea (blue).

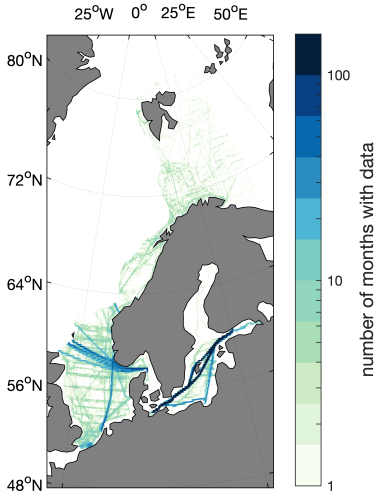

Figure 2. The number of months with fCO_2 data from SOCAT v5 in each grid box. The data cover a range of20 years (240 months).

The pCO_2 value of the respective open ocean maps ~~(~~was used for MLR 1 and MLR 2~~), or the year were added (MLR 3).~~ , while year was always used as a driver variable in MLR 3. Inclusion of stationary drivers (such as month, latitude and longitude) in the MLR increased the performance of MLR 2 and MLR 3. However, these were still not better than MLR 1 and we therefore decided to limit this analysis to dynamic parameters. Using dynamic drivers only, assures a dynamic description of the conditions in the field, and gives us the possibility to reproduce changes caused by a regime shifts, for example the ongoing ~~atlantiefication~~ atlantification of the Barents Sea (Oziel et al., 2016; Lind et al., 2018).

2.4 Validation

The three linear fits were compared to each other in each region by taking into account the R^2 and the root mean square error (RMSE) of the fit, and the Nash Sutcliffe method efficiency (ME) (Nondal et al., 2009). The method efficiency compares how well the model output (E_n) fits the observations (I_n) for every data point n to how well a simple monthly average ($\bar{I}$) would fit the observations:

$$\mathrm{ME} = \frac{\sum_n (I_n - E_n)^2}{\sum_n (I_n - \bar{I})^2} \quad (2)$$

A method efficiency >1 means that using just monthly averages of all data in the region would fit better to measured data than the respective model~~,~~. Generally, a method efficiency >0.8 is considered bad. Besides the statistics of the fit itself, the final maps were also compared to the gridded SOCAT v5 data, resulting in an average offset and standard deviation. In order to compare the maps against data that were not used to produce the maps, we predicted the fCO_2 for the years 2017 and 2018 (~~ie~~i.e., we applied the trained multi-linear model to driver data from 2017 and 2018) and compared these maps to fCO_2 observations in

Table 4. Driver used in the different regressions.

	~~MLD~~log (MLD)	SST	SSS	CHL	ICE	ICE change	~~BAT~~log (BAT)	DIST	pCO_2	year
North Sea										
MLR 1	x	x	x	x	x		x		x	
MLR 2	x	x	x	x	x	x	x	x	x	
MLR 3	x	x	x	x	x	x	x	x		x
Norwegian Coast										
MLR 1	x	x	x	x	x		x		x	
MLR 2	x	x	x	x	x	x	~~x~~		x	
MLR 3	x	x	x	x	x	x	x			x
Barents Sea										
MLR 1	x	x	x	x	~~x~~	x	x		x	
MLR 2	x	x	x	x	x	x	~~x~~		x	
MLR 3	x	x	x	x	x	x	~~x~~			x
Baltic Sea										
MLR 1	x	x	x	x	x	x	x		x	
MLR 2	x	x	x	x	x	x	~~x~~		x	
MLR 3	x	x	x	x	x		x			x

SOCAT v2019, gridded on a monthly 0.125°x0.125° grid. We also compare the ~~map~~ maps directly with observations ~~at two time series~~ from repeated sampling locations in the North Sea and the Baltic Sea.

2.5 Ocean acidification

For calculating ~~ocean acidification~~the pH, alkalinity (AT) was estimated in the North Sea, along the Norwegian Coast, and in the Barents Sea via a salinity-alkalinity correlation after Nondal et al. (2009). Alkalinity describes the capacity of the sea water to buffer changes in pH. As the concentration of most of the weak ~~acids~~ bases in seawater is strongly dependent on the salinity, alkalinity can in many regions be estimated from salinity. However, in regions with a high amount of organic ~~acids~~ bases in seawater, for example in strong blooms or at river ~~moths~~mouths, deviations from the alkalinity-salinity relationship can ~~be observed~~occur. The carbonate system was calculated using the CO2SYS program (van Heuven et al., 2009) with carbonic acid dissociation constants of Mehrbach et al. (1973) as refitted by Dickson and Millero (1987)~~and~~ , KSO_4^- dissociation constants after Dickson (1990) and the boron-salinity relation after Uppström (1974). For the Baltic Sea, we did not calculate pH as the alkalinity-salinity relationship in this region is complex due to different AT-S relations in different sub-regions of the Baltic Sea, and a non-negligible increase of AT over the last 25 years (Müller et al., 2016).

2.6 Calculation of trends

For calculating trends of fCO_2 and ocean acidification, the data in every grid box were deseasonalised by subtracting the long-term averages of the respective months. Then a linear fit was applied to the deseasonalised time-series. For illustrating the influence of interannual variability we calculated the trend for different time ranges. As a time range less than 10 years barely resulted in significant trends, we decided to limit the trend analysis to starting years ~~from~~ 1998 ~~to~~ through 2006 and ending years ~~from~~ 2008 ~~to~~ through 2016.

2.7 Flux calculation

The air-sea disequilibrium was calculated as the difference between our mapped fCO_2 values and atmospheric fCO_2 in each grid cell and time step. The atmospheric fCO_2 was determined by converting the xCO_2 from the NOAA Marine Boundary Layer Reference product from the NOAA GMD Carbon Cycle Group into fCO_2 by using ~~the~~ monthly SST and SSS data (Table 3) and monthly air pressure data from the NCEP-DOE Reanalysis 2 ~~(?)~~(Kanamitsu et al., 2002). We calculated the air-sea CO_2 flux (F) according to Equation 3, such that negative fluxes are into the ocean. The gas transfer coefficient k was determined using the quadratic wind speed (u) dependency of Wanninkhof (2014) (Equation 4). The Schmidt number, Sc, was calculated according to Wanninkhof (2014) and the solubility coefficient for CO_2, K_0, after Weiss (1974).

$$\mathrm{F} = k \cdot K_0 \cdot (fCO_{2,\mathrm{sw}} - fCO_{2,\mathrm{atm}}) \tag{3}$$

$$k = a_q \cdot \langle u^2 \rangle \cdot \left(\frac{Sc}{660}\right)^{-0.5} \tag{4}$$

In our calculations, we used 6-hourly winds of the NCEP-DOE Reanalysis 2 product. The coefficient a_q in Equation 4 is strongly dependent on the used wind product (Roobaert et al., 2018). We determined it to be ~~$a_q = 0.16 \mathrm{cm\,h^{-1}}$~~ $a_q = 0.16$ cm $\mathrm{h^{-1}}$ for the 6-hourly NCEP 2 product following the recommendations of Naegler (2009) and by using the World Ocean Atlas sea surface temperatures (Locarnini et al., 2018). The barrier effect of sea ice on the flux was taken into account by relating the flux to the ~~degree of ice cover following of~~ ice cover extent following Loose et al. (2009). As the gas exchange in areas that are considered 100% ice covered from satellite images should not be completely neglected, we use a sea ice barrier effect for a 99% sea ice cover in all grid cells where the sea ice coverage exceeded 99%.

3 Results

3.1 Maps of fCO_2

The skill assessment metrics for MLR 1, MLR 2 and MLR 3 are presented in Table 5. It shows the the R^2 and RMSE of the fit, the ME, as well as the average offset and standard deviation to the gridded SOCAT data. The coefficients for MLR 1, MLR 2 and MLR 3 are provided in the supplement. The MLRs substantially improve the predictions of the open ocean maps in all

studied regions, showing a better average offset and standard deviation to SOCAT v5 and ME than the coarser-resolution open ocean maps (for example: Rödenbeck map: North Sea 0 ± 95 μatm, Norwegian Coast: 2 ± 17 μatm, Barents Sea: 22 ± 40 μatm, Baltic Sea: 4 ± 48 μatm; ~~MLD1~~MLR1: North Sea: 0 ± 26 μatm, Norwegian Coast: 0 ± 16 μatm, Barents Sea: 0 ± 19 μatm,Baltic Sea: 2 ± 42 μatm). In all regions MLR 1 ~~was performing best, showing also~~ has the best model efficiency, the highest R^2 and the smallest RMSE of the fit, while these statistics are worse for MLR 2 and MLR ~~3 showed a weaker performance.~~ 3. This can be explained by the fact that the Rödenbeck map contains ~~also~~ information about the ~~coasts~~ continental shelf and the Barents Sea, while for MLR 2 the closest open ocean grid cell of Landschützer et al. (2017) was used. The fact that MLR 3 showed the weakest performance ~~, which~~ shows the value of using information from the open ocean maps in the regression.

Figure 3 shows, from left to right, the spatial distribution of the average difference between the predicted fCO_2 by ~~MLR1~~ MLR 1 and the gridded SOCAT v5 data, the Rödenbeck map and the gridded SOCAT v5 data, the difference between MLR 1 and the Rödenbeck map, and, for comparison, between MLR 3 and the SOCAT v5 data. In the North Sea, MLR 1 seems to slightly overestimate the fCO_2 in the constantly mixed region at the entrance of the English channel and the area off the Danish North Sea coast. In the Baltic, MLR 1 generally describes ~~well~~ the spatial variability in fCO_2 ~~. In~~ well. However, in the Gulf of Finland it usually predicts too low fCO_2 values during May/June while ~~MLR 1~~ it slightly underestimates events of very high fCO_2 in December/January. ~~However, it shows lower spatial biases than~~ Regardless, the spatial biases vs SOCAT are clearly smaller for MLR 1 than for the original Rödenbeck map. ~~MLD~~ Further, as the predictions of MLR 2 and 3 are ~~showing much larger differences from SOCAT v5 data, especially in the Baltic Sea and the southern North Sea. Therefore~~clearly inferior to those of MLR 1 (Table 5 and Figure 3 (MLR 3 only)), we will use MLR 1 ~~in the further analysis~~results for the further analyses. An extended validation of the MLR 1 maps can be found in the discussion section.

Figure 4 shows the monthly averages of fCO_2 produced by MLR 1 for February, May, August and November. In all regions, the highest fCO_2 values occur in the winter, while the lowest fCO_2 occur in summer. The largest seasonal cycle could be observed in the Baltic Sea, where fCO_2 reached well below 200 μatm in mid summer and over 500 μatm during the winter.

We notice that the gradients that exist between the grid cells in the Rödenbeck map, are still visible in our maps in some regions, for example the sharp gradient in the southern North Sea in February, or the east-west and north-south gradients in the entire North Sea in August. Such gradients are also evident in directly mapped pCO_2 data (Kitidis et al., 2019), however, here they are strongly meridional and latitudinal in their extent. As such, while these gradients do reflect actual features of the fCO_2 distribution in the North Sea, their specific shape here, are also a consequence of the influence of the Rödenbeck maps on our estimates; from the use of these maps as a driver in the MLR and their importance in improving the statistical performance vs the MLR that did not use these values as a driver (MLR 1 vs MLR 3, Table 5). Also, they do reflect the uncertainty of - and our level of confidence in - the estimated pCO_2 values; being approximately similar to or slightly larger than the RMSE of MLR 1 (Table 5). Any smoothing would be completely artificial, and, while being more visually pleasing, would not better reflect the truth in any meaningfully quantifiable extent. We have therefore chosen to leave them untouched. These gradients are therefore also visible in subsequent pH and trend maps.

Table 5. Statistical evaluation of the MLR 1, MLR 2 and MLR 3 in comparison to the open ocean maps of Rödenbeck et al. (2015) and Landschützer et al. (2017) for each region. The data for the open ocean map of Landschützer et al. (2017) are in parentheses since this is based on an extrapolation of ~~he closed~~ the nearest open ocean grid cell towards the coast. The number of grid cells containing data is given behind the region abbreviations.

	R^2 adj	RMSE	ME	difference to gridded SOCAT v5	
			median	mean	standard deviation
		/μatm		/μatm	/μatm
North Sea (36170)					
MLR 1	0.7271	25	0.3145	-0.15	26
MLR 2	0.5130	33	0.5789	-0.52	36
MLR 3	0.5331	33	0.4895	-2.4	32
Rödenbeck			0.3522	-0.28	95
(Landschützer)			0.5714	-4.7	103
Norwegian Coast (16014)					
MLR 1	0.7860	16	0.1742	0.46	16
MLR 2	0.5634	22	0.3597	-2.3	24
MLR 3	0.6074	20	0.2436	-0.08	21
Rödenbeck			0.2177	2.0	17
(Landschützer)			0.3294	7.0	23
Barents Sea (13925)					
MLR 1	0.8871	12	0.1069	0.32	19
MLR 2	0.8724	14	0.0986	1.3	68
MLR 3	0.8672	18	0.1082	1.3	24
Rödenbeck			0.2923	22	40
(Landschützer)			0.3364	15	44
Baltic Sea (46810)					
MLR 1	0.9076	39	0.0488	2.2	42
MLR 2	0.6733	66	0.3111	-1.0	68
MLR 3	0.6628	67	0.3027	0.24	69
Rödenbeck			0.1326	4.2	48

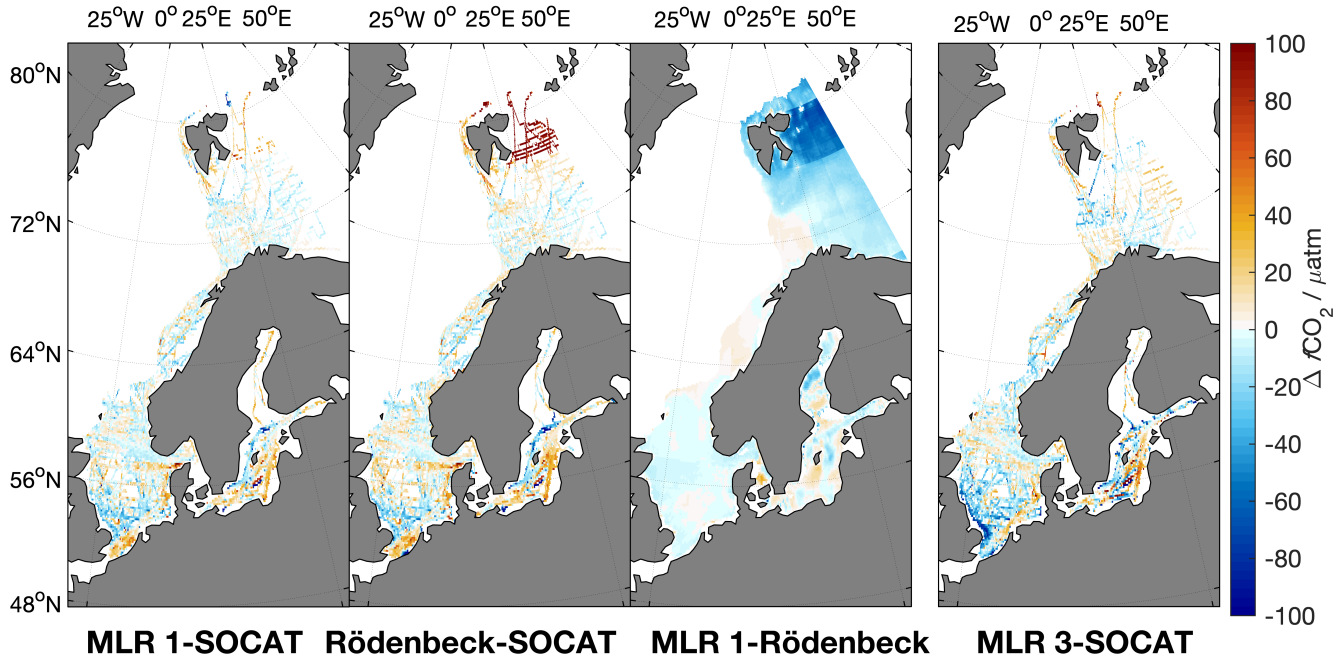

Figure 3. Average regional differences between MLR 1 and gridded SOCAT v5 data, the Rödenbeck map and gridded SOCAT v5 data, MLR 1 and the Rödenbeck map, and MLR 3 and the gridded SOCAT v5 data (from left to right).

3.2 Maps of pH

The monthly average of pH calculated from MLR 1 fCO_2 ~~is ranging~~ ranges from about 8 during winter to 8.15 during summer in the North Sea and at the Norwegian coast (Figure 5). Towards the Barents Sea the pH maximum ~~increases during summer~~ during summer increases to 8.2. The pH of 8.00 - 8.15 in regions with a large influence from the Atlantic, such as the northern North Sea and the Norwegian coast, is in good agreement with the range of pH determined for the open North Atlantic (Lauvset and Gruber, 2014; Lauvset et al., 2015). In the North Sea, the pH is in the same range as reported in Salt et al. (2013) and it also shows the same distribution in August/September, with higher pH in the northern North Sea and lower pH in the southern part.

4 Discussion

4.1 ~~Validation~~ Performance of the pCO_2 maps

The performance of the MLR and the ~~produced~~ maps are evaluated in different ways: (1) the R^2 and the RMSE of the fit~~between the driver data and the gridded observations~~, (2) the average deviation and its standard deviation, as well as the ME between

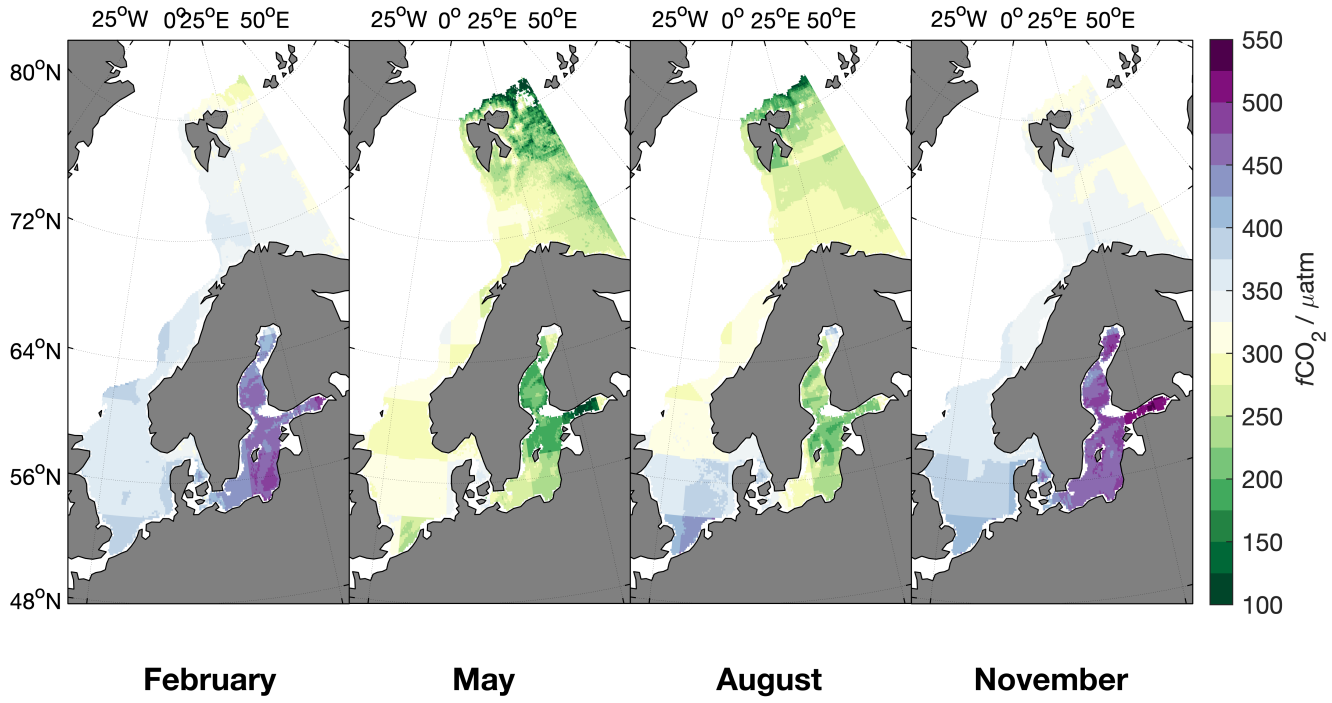

Figure 4. The average fCO_2 of MLR 1 (1998-2016) for one example months in each season (February, May, August and November).

the produced fCO_2 maps and the gridded observations as a regional average, (3) showing the median deviation between the MLR and the gridded observations on a monthly level, and (4) by comparing the data from the fCO_2 maps to observations from two time series stations. (2) - (4) will be shown for ~~both,~~ the time period covered by the driver data (1998-2016) and ~~a~~ for the prediction of the ~~maps into the years~~ fCO_2 values for 2017 and 2018. These predicted values are compared with data from the newest SOCAT release (SOCATv2019) and provide a comparison with an independent dataset. Please note that the comparability of the model performance between the different regions is limited. All used statistical parameters are influenced by characteristics that can vary substantially between the different regions, such as range of the data, their variability or the amount of grid cells with data. ~~Additionally~~For example, in a diverse region with many measurements the amount of variability captured by these measurements is most likely larger and, thus will lead to a weaker correlation.

Generally, the uncertainty of MLR 1 ~~are~~ is in the same range as in other studies (Laruelle et al., 2017; Yasunaka et al., 2018) mapping coastal fCO_2 dynamics: 25 μatm in the North Sea, 16 μatm along the Norwegian Coast, 12 μatm in the Barents Sea,

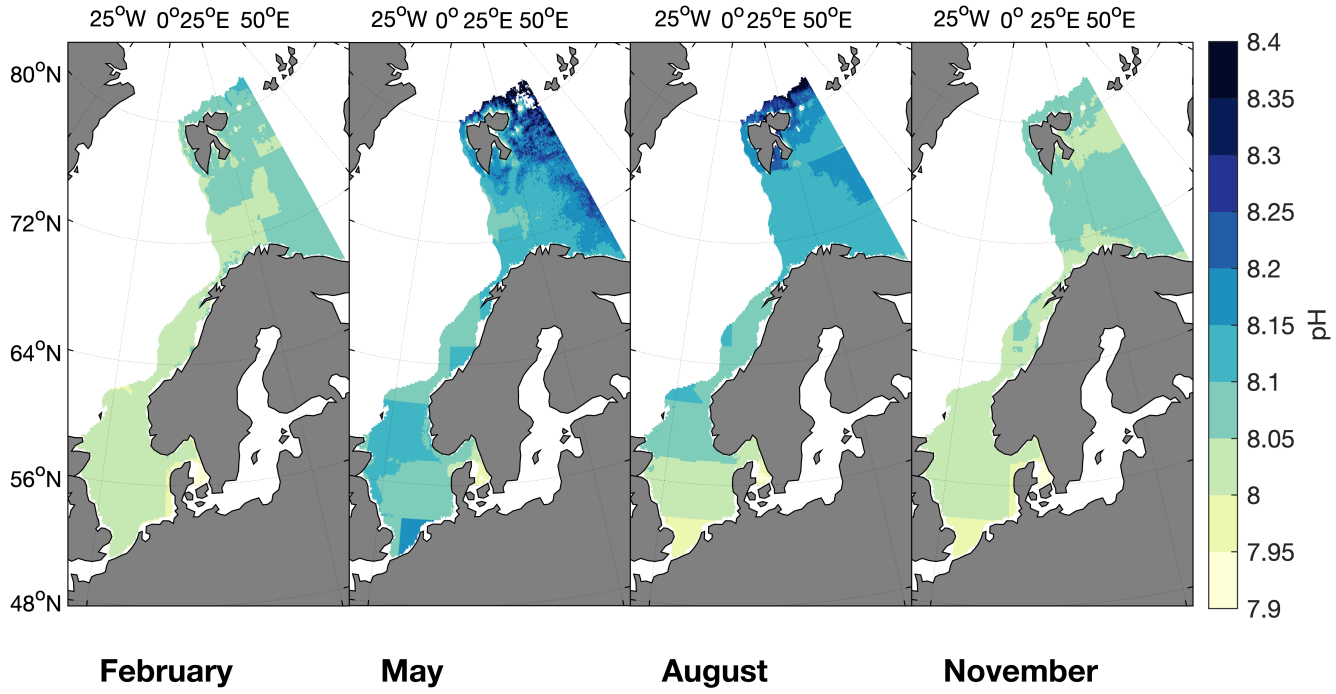

Figure 5. The average pH based on MLR 1 (1998-2016) for one example month in each season (February, May, August and November).

and 39 μatm in the Baltic Sea (based on the RMSE in Table 5). In the Baltic Sea, which has a large variability in itself, Parard et al. (2016) obtained lower standard deviations through dividing the area in smaller sub-regions.

One clear drawback of the here presented MLR 1 is the clearly visible grid-pattern of the open ocean pCO_2 product that was used as input data with its grid size of 5 x 4 °, mentioned in Sect 3.1. There are two ways how one could get rid of this artifact in a future release. A finer resolution of the used open ocean maps will lead to a better representation of the actual gradients in our mapped product. Rödenbeck et al. just released a newer, finer resolution of their open ocean product (2.5 x 2°) that we intend to use in a future version of this data product. However, this will not be sufficient to eradicate the artifact completely. Another approach, running the MLR without an open ocean pCO_2 product can provide a coastal pCO_2 product without this artifact. While in principle it is preferential to have coastal maps that are independent of the open ocean products, MLR 3, which is running without open ocean pCO_2 as driver, did clearly not reach the same accuracy as MLR 1 (Table 5). New and better input fields or a different regression method could help improving the independent coastal maps in the future.

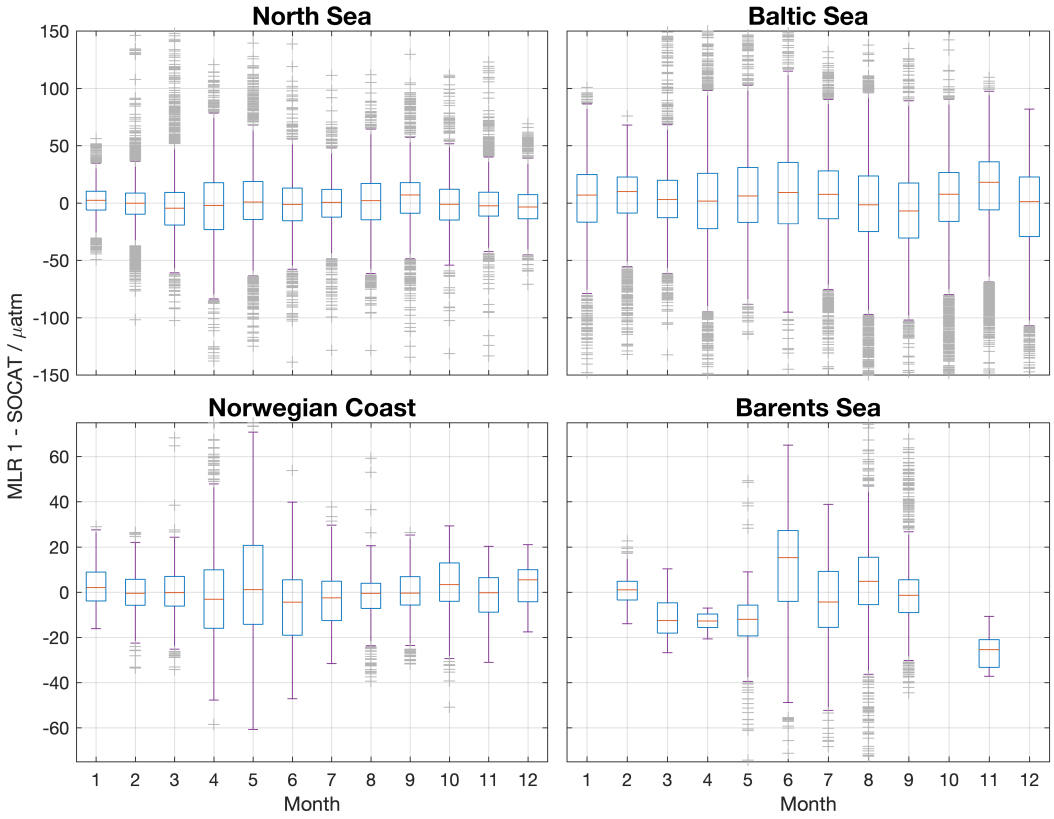

Figure 6. Boxplots showing the median deviation of MLR 1 from the gridded SOCAT ~~v5~~ 5 data for each region (red line). The boxes show the ~~respective~~ upper and lower 75% percentiles. 99% of the data lays within the range of the purple whiskers. Extremes are shown as gray crosses.

The seasonal differences between MLR 1 determined values and the SOCAT v5 data for each region are shown in Figure 6. This comparison shows a very good agreement. For MLR 1, the seasonal variations of the median bias are small in the North Sea, along the Norwegian coast and in the Baltic Sea. In the Barents Sea, however, the bias varies seasonally. Here, MLR 1 slightly underestimates the fCO_2 in winter and early spring, while it overestimates the fCO_2 in summer. In all other regions, the median seasonal bias is smaller than the uncertainty of the maps. The larger seasonal bias in the Barents sea is most likely caused by the larger seasonal bias in the number of available observations. There ~~is~~ are no data available in October, December and January.

When comparing all observations from the years 2017 and 2018 to the predictions by the ~~MLR1~~MLR 1, we find a good agreement in the North Sea (2 ± 20 μatm) and no seasonal bias (Figure 7). In the other regions, the agreement is somewhat reduced compared to the years ~~1998-2016~~ 1997-2016 (-9 ± 39 μatm (Norwegian Coast), -5 ± 29 μatm (Barents Sea) and 28 ± 58 μatm (Baltic Sea)). In these regions we also observe a seasonal bias in the years 2017 and 2018. At least for the Baltic

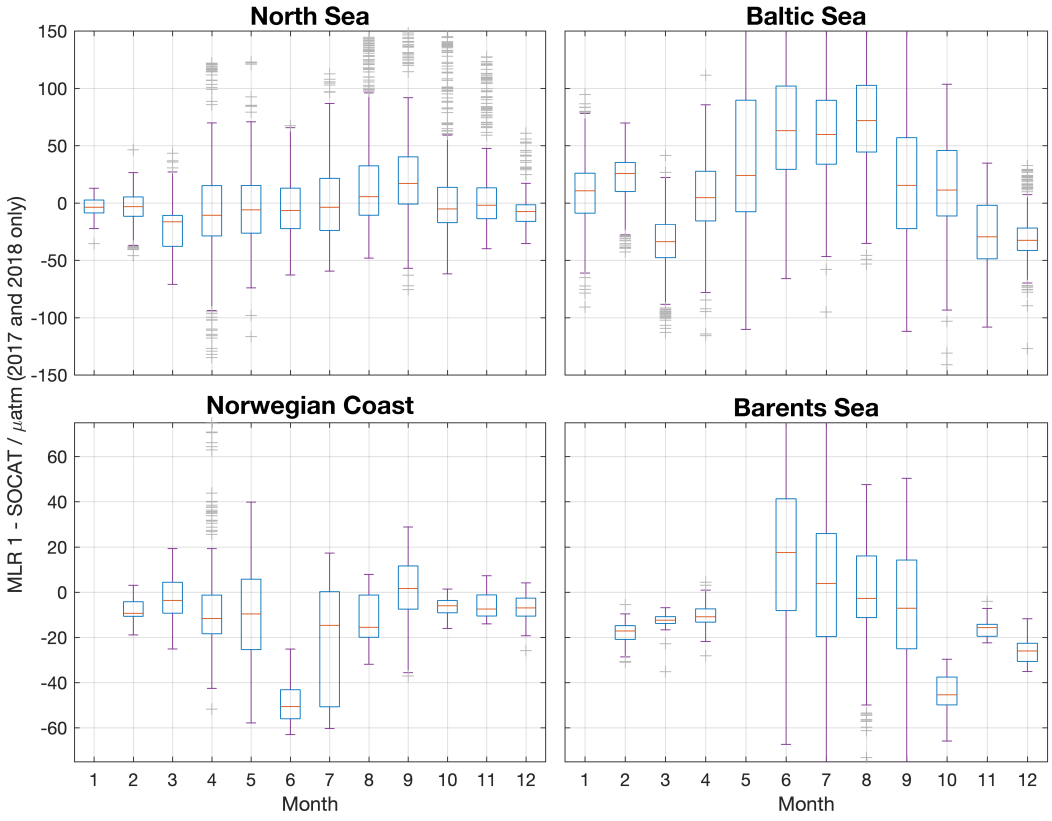

Figure 7. Boxplots showing the median deviation ~~of~~ between MLR 1 (based on observations until 2016) ~~predicted~~ and measured fCO_2 values in 2017 and 2018. The boxes show the ~~respective~~ upper and lower 75% percentiles. 99% of the data lays within the range of the purple whiskers. Extremes are shown as gray crosses. The number of grid cells with data available were: North Sea: 5047, Norwegian Coast: 1543, Barents Sea: 2312, Baltic Sea: 5414.

Sea this could be a ~~reason of a extraordinarily~~ result of the extraordinary warm and dry summer in 2018, that ~~lead~~ led to very low fCO_2 values ~~in the Baltic Sea Bakker et al. (2016) Please note~~(see Figure 8 and the data in SOCAT (Bakker et al., 2016)). Please note, that for this comparison ~~,~~the MLR was extrapolated in time. Only observations until December 2016 were used to produce the MLR. Therefore accuracy of the maps itself is reduced.

In a second test to investigate to which extent MLR 1 can reproduce observations we compared the MLR output with time series data from two voluntary observing ship lines in two very different regions with a good data coverage: M/V Nuka Arctica in the northern North Sea (0-2°E, 58-60°N) and M/V Finnmaid in the Baltic Sea (23-24°E, 59-60°N) (Figure 8). ~~To every observation we assigned the related value of MLR 1.~~ The agreement between the MLR 1 and the observations is very good. MLR 1 reproduces the general seasonality and some of the interannual variability, also in the years 2017 and 2018, of which the observations were not used in the regression.

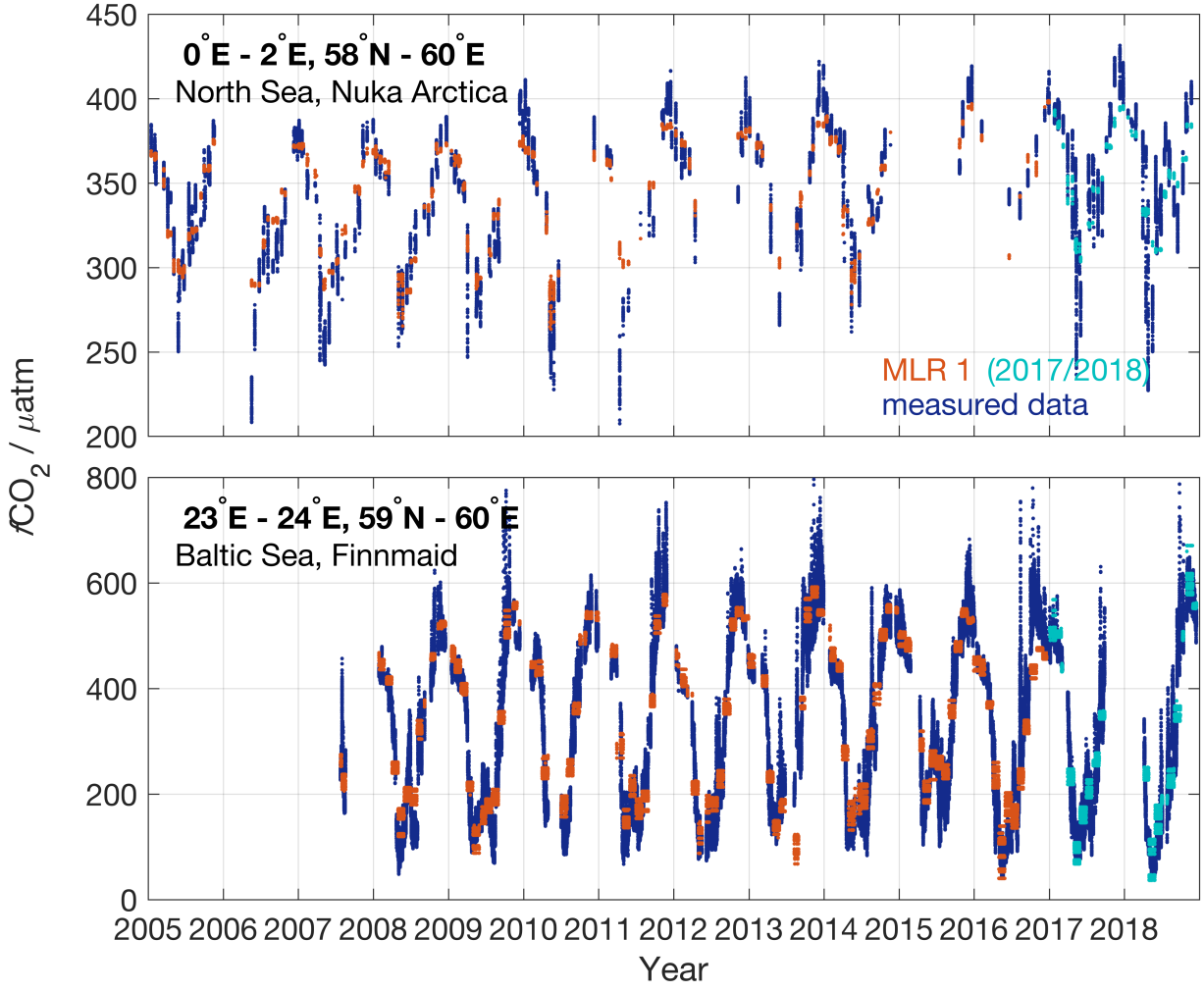

Figure 8. Time series of VOS data from Nuka Arctica (upper panel, blue) and Finnmaid (lower panel, blue) compared with MLR 1 at the same location (red). In light blue the predictive MLR output for the years 2017 and 2018 is shown.

When performing interpolation exercises it is always important to be aware of the fact that the resulting maps might come with biases and do not represent all regions equally well. While the here presented maps give a good general overview about the surface ocean fCO_2 variability in regions with a relatively large amount of data, the reliability, however, is limited in ~~those~~ regions where the data coverage is more scarce. This is especially the case, when the region with scarce data coverage is showing different characteristics in, for example, temperature and salinity, compared to the rest of the region. One such example is the Gulf of Bothnia in the Baltic Sea region where almost all data used to derive the MLR is from south of 60°N i.e. not in the Gulf of Bothnia, but in the Baltic Proper and western Baltic Sea (see Figure 2). The MLR method can also lead to unrealistic extreme values and even negative fCO_2. Some such values occur in the northeastern Barents sea as well as in ~~some~~ parts of the Baltic Sea (about 0.01% of the grid cells in each region). As pH cannot be calculated for negative fCO_2, we excluded all negative fCO_2 values for the calculation of pH. Excluding the negative values resulted in a change of the average fCO_2 of 0.05 μatm (Baltic Sea) and 0.3 μatm (Barents Sea) so they are of negligible importance for the flux estimates. While the negative values are easy to spot and discard there are most likely ~~more~~ other unrealistically low values in spring and summer ~~data~~ in the very north and northeastern Barents Sea as well as some parts of the Baltic Sea. However, there are no data available in SOCAT v5 or elsewhere available to validate this~~to validate this~~.

All regions with questionable fCO_2 are also questionable in their pH data. There is a number of very high pH in the Barents Sea (Figure 5), that are associated with also very low fCO_2 (4) that might not be realistic. In addition, estimated pH values in ~~regions or seasons~~ low salinity regions where the actual alkalinity-salinity deviates strongly from the Nondal et al. (2009) one used here (e.g. river mouths in the southern North Sea or the Skagerrak), should be interpreted with caution.

4.2 Trends in fCO_2 and pH

~~The trends~~ Trends in surface ocean fCO_2 in coastal regions are often difficult to assess because of the scarcity of ~~the~~ data relative to the highly dynamical character of these regimes and their large interannual variability. ~~One issue is that~~ For example, the start of the productive season can range from February to April even within a small area, such that even restricting the analysis to specific seasons (e.g. winter) can be challenging. ~~However~~Also, due to lack of data, especially winter data, most observational studies are based on ~~repeated sections during summer~~ summer data. Further, the fact that these measurements typically do not take place every year, adds even more uncertainty to the estimated trend, as ~~the~~ interannual variability can mask the trend signal.

The monthly maps of fCO_2 from 1998 to 2016 enable us now to estimate the trend in surface ocean fCO_2 for the entire region~~and~~, equally distributed over the seasons (Figure 9, left). All trends were computed ~~by using~~ from deseasonalized data. The interannual variability of the trend estimates in each region is shown in the panels on the right hand side in Figure 9. We exclude the northern Baltic Sea from the trend map because we do not expect to have a robust trend estimate in that region as there are only very few data from that region in the regression. Based on the linear regression the significant trends in fCO_2 have an average uncertainty of 0.5 μatm/yr (North Sea), 0.4 μatm/yr (Norwegian Coast), 0.4 μatm/yr (Barents Sea), and 0.7 μatm/yr (Baltic Sea), while the shorter time periods shown have a higher~~and the~~, no longer time periods ~~a lower uncertainty~~than 1998-2016 (for which the given uncertainties of the trend apply) are shown. For pH trends~~the average uncertainty of the~~

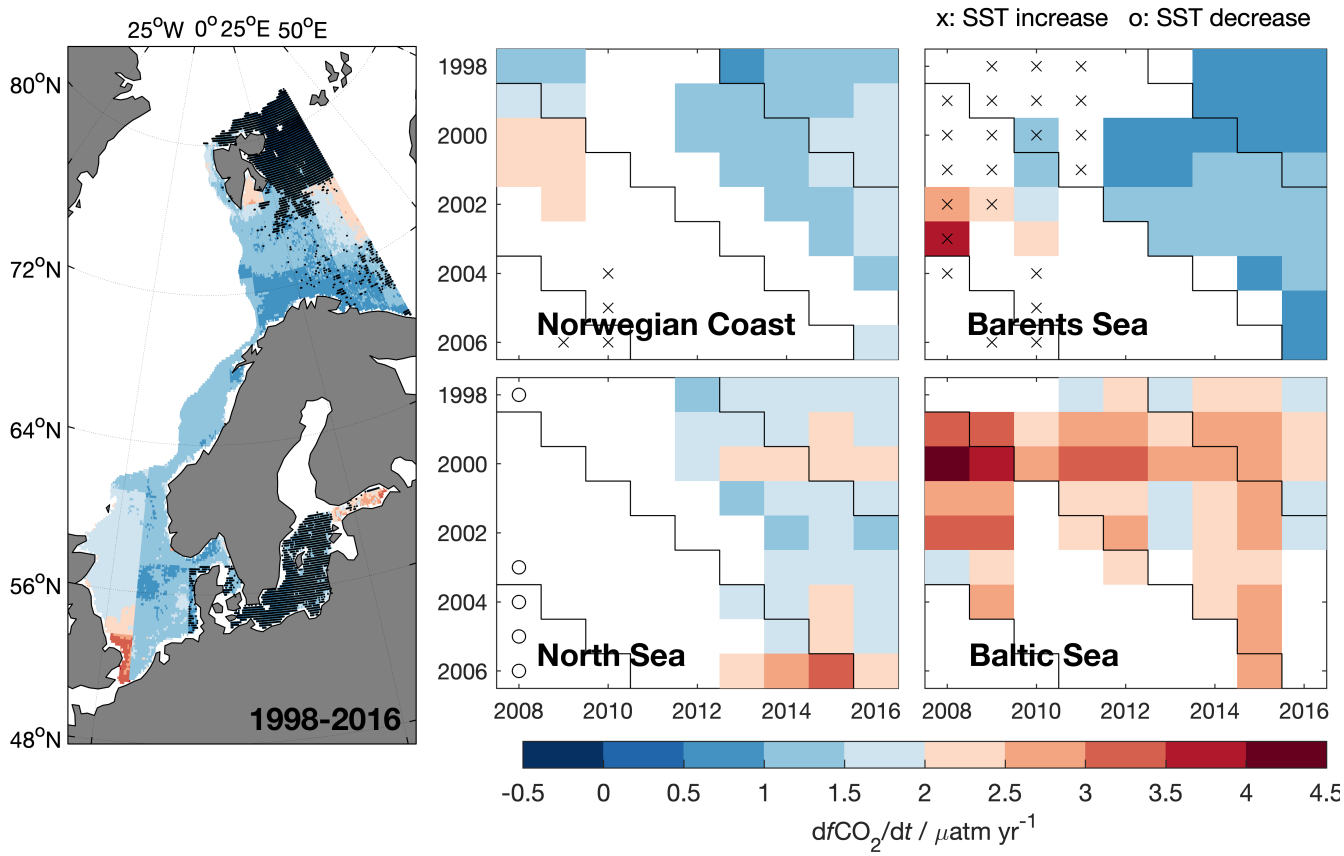

Figure 9. The trend in surface ocean fCO_2 estimated from deseasonalized fCO_2. The left hand panel show the spatial distribution of the trend over the time period from 1998 to 2016. Grid boxes without a significant trend are denoted with a black dot. ~~On the~~ The four right hand panels show the ~~influence of the~~ trends in different time ~~range~~ periods in four regions, from the various years on the ~~average trend is shown for~~ y-axis to the ~~four regions~~various years on the x-axis. Non significant trends were left blank. Significant trends in sea surface temperature are indicated with crosses/circles. The colorbar is centered on the approximate annual fCO_2 rise in the atmosphere (2 μatm/yr)

~~regression is~~ , the average uncertainties of the regressions over 1998-2016 are $5 \cdot 10^{-4}$ (North Sea) and $7 \cdot 10^{-4}$ (Norwegian Coast and Barents Sea).

~~The trend in surface ocean pH estimated from deseasonalized pH. On the left hand the spatial distribution of the trend over the time period from 1998 to 2016 is shown. Grid boxes without a significant trend are denoted with a black dot. On the right hand the influence of the time range on the average trend is shown for the four regions. Non significant trends were left blank.~~

In most of the regions addressed in this study, the trend in the surface ocean is lower than the trend in atmospheric xCO_2 (global average 2.02 ppm yr $^{-1}$ ("Cooperative Global Atmospheric Data Integration Project", 2015)). Trends exceeding the atmospheric values in the period from 1998 to 2016 can only be observed at the entrance of the English Channel, in Stor-

Table 6. fCO_2 trend calculated from gridded, deseasonalized SOCAT v5 observations.

Region	Latitude / °N	Trend / μatm yr^{-1}
North Sea, South	51 - 54.5	3.2 ± 1.3
North Sea, Center	54.5 - 58	1.43 ± 0.21
North Sea, North	58 - 62	2.320 ± 0.089
Norwegian Coast, South	62 - 68	2.12 ± 0.19
Norwegian Coast, North	68 - 73	1.426 ± 0.099
Barents Sea, South	69 - 74	1.31 ± 0.30
Barents Sea, North	74 - 85	1.01 ± 0.22
Baltic Sea, South	54 - 56	2.05 ± 0.12
Baltic Sea, North	56 - 61	1.84 ± 0.21

fjorden/Svalbard ~~, the Gulf of Finland~~ and the Gulf of ~~Bothnia~~ Finland ($2.5 - 3$ μatm yr^{-1}). It has to be noted that there was almost no measured fCO_2 as MLR input ~~in neither Storfjordennor the Gulf of Bothnia~~from Storfjorden. Therefore, these trends ~~should be handled with care. The~~ are highly uncertain. The trend in the western North Sea ~~has a trend that~~ is only slightly lower than the trend in the atmosphere ($1.5 - 2$ μatm yr^{-1}), while the trends in the eastern North Sea, along the Norwegian coast and in the Barents Sea are ~~somewhat~~ lower (0.5-1.5 μatm yr^{-1}). In the North Sea this is consistent with a recent study of Omar et al. (2019), which is directly based on observations~~Omar et al. (2019). The low trends~~ . These low trends will result in an increase in the strength of the ocean carbon sink with time. ~~A trend smaller than the atmospheric trend can be caused by a shift in the bloom onset. For example, in the North Sea a significant drawdown in~~

Generally, only few regressions over time ranges of less than 10 years turned out to be significant. This is an important finding when comparing the trends determined from our maps with the trends reported in literature, of which many were covering periods shorter than 10 years (Table 1). In order to compare the general patterns of fCO_2 ~~has been observed as early as February in some years (Omar et al., 2019). The bloom onset in the North Sea after the 1990s has been shown to be mainly triggered by the spring-neap tidal cycle and the air temperature by Sharples et al. (2006). They found that the onset of spring bloom has occurred on average 1 day earlier every year. Over the period covered in this study (almost 20 years)this could cause a change of three weeks in the timing of the spring bloom. Even if the trend in winter~~ trends determined from our maps with those directly determined from observations over a similar time range, we estimated the fCO_2 ~~was following the atmospheric xCO_2 increase, such a change in bloom onset would lead to a trend lower than the atmospheric when averaging over the entire year.~~ trends also from the SOCAT v5 observations that were used to produce the MLR (Table 6). We gridded and deseasonalized the SOCAT v5 data and divided the entire region into 9 subregions. A figure showing the fits and the data coverage can be found in Appendix A. These observation based trends show similar general patterns as those based on our

maps (Figure 9, 1998-2016): (1) largest trends in the southern North Sea, (2) decreasing towards the north with trends around the atmospheric trend in the northern North Sea and trends around 1 μatm yr^{-1} in the Barents Sea, (3) close to atmospheric trends in the Baltic Sea.

The observation that ~~large~~ some subareas (the Baltic Sea ~~, the~~ or along the shore of the western North Sea) did not show a significant trend can be explained by the fact that ~~, coastal~~ coastal sea systems, especially enclosed areas as the Baltic Sea, experience a high anthropogenic pressure. Anthropogenic impacts other than rising atmospheric CO_2 concentrations ~~influencing~~ influence the ocean carbon system~~and the bloom properties such as the~~ , for example the nutrient load of rivers can effect coastal ecosystems ~~through eutrification, resulting~~ and primary production through eutrophication. This will result in lower fCO_2 in summer and higher fCO_2 in winter (Borges and Gypens, 2010; Cai et al., 2011). Another important process that influences the carbon system in the Baltic Sea are inflow events from the North ~~sea~~Sea. In between such events, CO_2 accumulates in deeper water layers causing an increasing gradient of dissolved inorganic carbon (DIC) across the halocline. Whenever deep winter mixing occurs, this will then lead to a large increase of surface fCO_2 because of the input of DIC rich waters from below. Another reason is the observed change in alkalinity with time~~which effects~~ . This affects the fCO_2 though changes in the buffer capacity of the inorganic carbon system (Müller et al., 2016).

In most other regions, the sea surface fCO_2 trends were typically smaller than the rise in the atmospheric CO_2 concentration. A possible explanation is an earlier onset of the spring bloom. For example, in the North Sea a significant drawdown in fCO_2 has been observed as early as February in some years, but there is also a large variability (Omar et al., 2019). The bloom timing and onset in the North Sea after the 1990s has been shown to be mainly triggered by the spring-neap tidal cycle and the air temperature (Sharples et al., 2006). The bloom timing and onset was found to be significantly earlier in the 2010s compared to the previous decades (Desmit et al., 2020). Even if the trend in winter fCO_2 was following the atmospheric xCO_2 increase, such a change in bloom timing and onset would lead to a trend lower than in the atmosphere when averaging over the entire year. Figure 10a shows the annual trends in fCO_2 in each month in the four regions considered. Particularly in the North Sea and Baltic Sea, very low fCO_2 trends are observed in February – May, suggesting that changing timing of the spring bloom might be important here. Investigating the seasonal fCO_2 in more detail (Figure 10b), revealed an earlier and deeper fCO_2 drawdown in the second decade of our analysis (2007-2016) than in the first (1998-2007) in the northeastern North Sea (58 – 60°N, 3 -8°E). This strongly suggest that an earlier and stronger spring bloom is lowering the annual fCO_2 growth rates in this region, which is among the ones with the smallest fCO_2 trends in the North Sea (about 1 μatm yr^{-1}, Fig. 9). In the other regions, no such changes could be established with confidence. Future investigations should aim at generating fCO_2 maps with higher temporal resolution, as changes in the timing of the spring bloom might be a matter of days or weeks, which would not be fully resolved by the monthly maps presented here.

When looking at the interannual variability, it becomes obvious that the trend in the North Sea is slightly smaller than the atmospheric CO_2 trend. In contrast, the Norwegian coast and the Barents Sea experience a robust trend much lower than the atmospheric trend (Norwegian Coast: $1 - 1.5$ μatm yr^{-1}, Barents Sea: around 1 μatm yr^{-1}). Here we can also see a stable pattern of warming over time scales of 10 to 15 years. The warming in itself would result in an increase of fCO_2 with time, in addition to the atmospheric forcing. As we are observing a trend smaller than the atmospheric trend, temperature effects

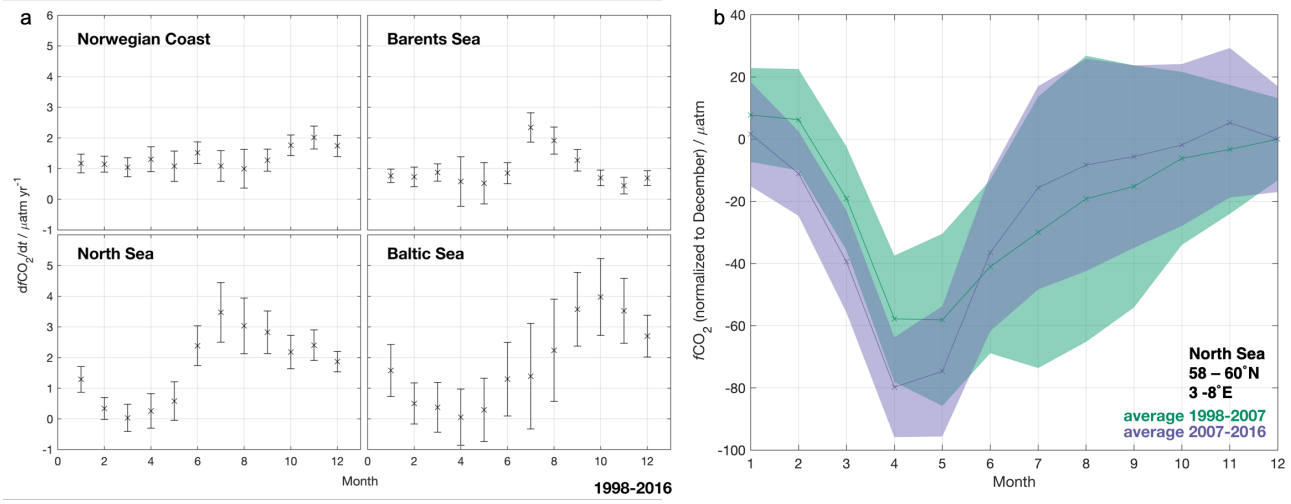

Figure 10. (a)The long term trend (1998-2016) in surface ocean fCO_2 each month. (b) The average seasonality in fCO_2 for the periods 1998-2007 (green) and 2007-2016 (purple) in the northeastern North Sea (58 - 60°N, 3 -8°E), normalized to December. The standard deviation for each month is shown as shaded area.

can't be the driver here. The lower trend stems most likely from an earlier onset of spring bloom. It has been shown that the atlantification and the reduced ice coverage of the Barents sea leads to a longer productive season, and this will result in more months with strong undersaturation in CO_2 (Oziel et al., 2016). In the Baltic Sea the pattens are different. Here the variability is much larger, while most of the time periods show a trend larger than the atmospheric trend ($3 - 3.5$ μatm yr^{-1}). Although slightly smaller our results broadly agree with trend estimates based on measurements of 4.6 - 6.1 μatm yr^{-1} over 2008-2015 (Schneider and Müller, 2018). Finally, it also needs to be noted that the uncertainty of the fCO_2 maps was highest in the Baltic Sea. This makes it also more difficult, if not impossible, to properly detect these small ~~trends.~~ differences in the trends.

For pH, the trend in most regions is around -0.002 yr^{-1} (Figure 11). A expected, regions with the strongest trend in fCO_2 also show the highest trend in pH, such as the southern North Sea. The trend in the northern North Sea and along the Norwegian Coast is in good agreement with the pH trends found in studies focusing on the open Atlantic Ocean (-0.0022 yr^{-1} (Lauvset and Gruber, 2014)) and the North Atlantic and Nordic Seas (-0.002 yr^{-1} (Lauvset et al., 2015)).

4.3 CO_2 disequilibrium and flux

The average ~~sea-air~~ air-sea CO_2 disequilibrium ($\Delta fCO_2 = fCO_{2,\mathrm{sea}} - fCO_{2,\mathrm{atm}}$) is shown in Figure 12. The only region showing an average supersaturation is the southern North Sea. Towards the north, the surface ocean becomes more and more undersaturated, with lowest values in the Barents Sea. The values ~~we found~~ in the Barents Sea (-60 to -80 μatm in the southern Barents Sea and less than -100 μatm around Svalbard) are in ~~generally in~~ agreement those estimated by Yasunaka et al. (2018).

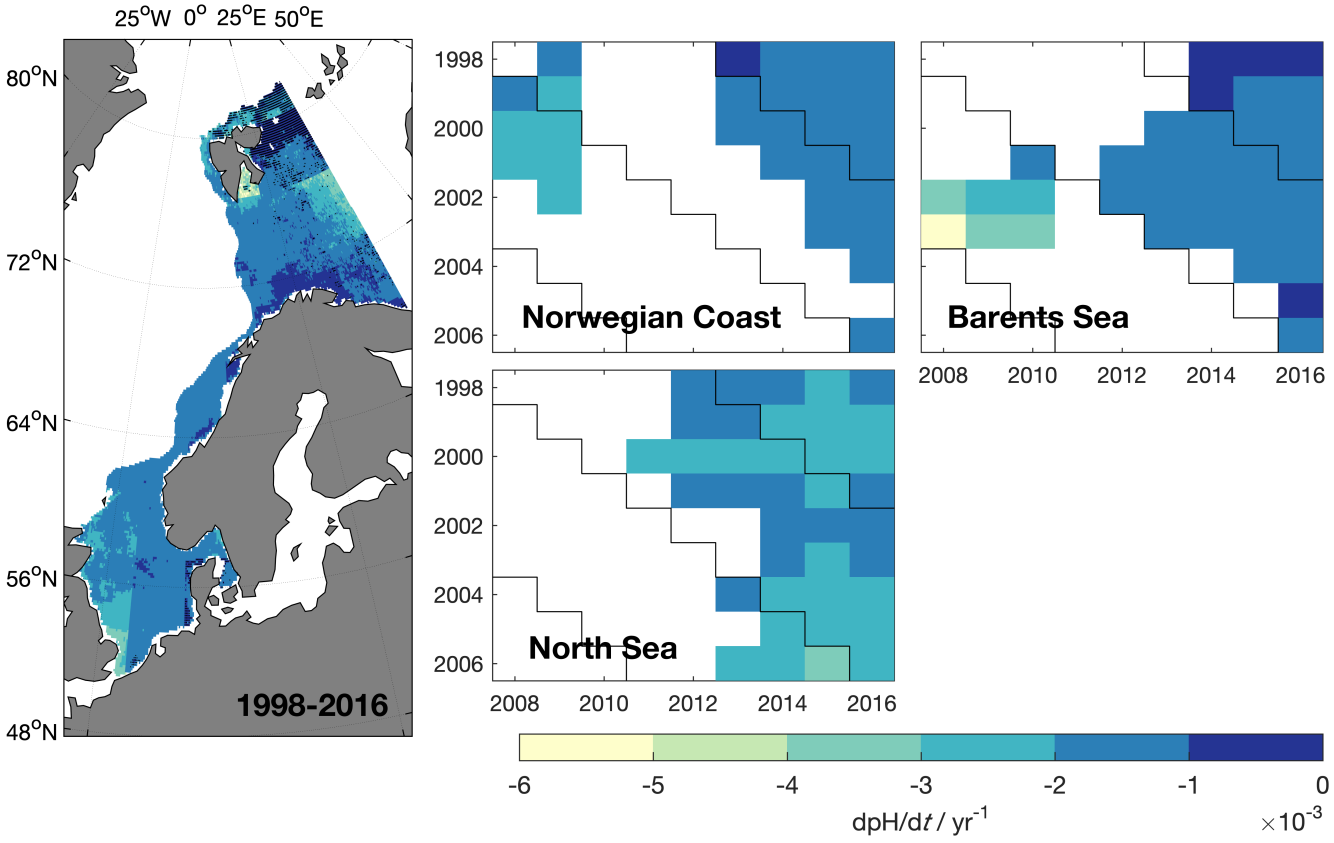

Figure 11. The trend in surface ocean pH estimated from deseasonalized pH. On the left hand the spatial distribution of the trend over the time period from 1998 to 2016 is shown. Grid boxes without a significant trend are denoted with a black dot. The three right hand panels show the trends in different time periods in three regions, from the various years on the y-axis to the various years on the x-axis. Non significant trends were left blank.

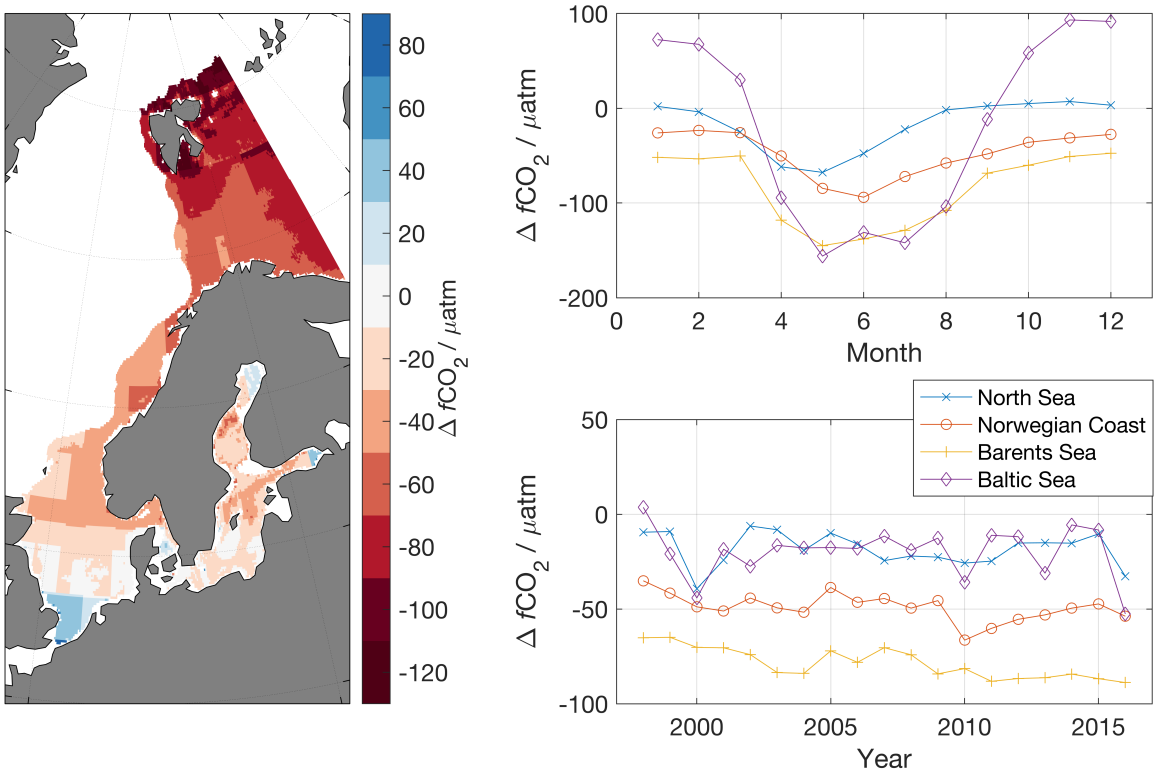

Figure 12. The average air-sea CO_2 disequilibrium over the period 1998-2016 (left hand panel, red colors indicate average undersaturation, while blue colors indicate average oversaturation). For every region average disequilibria are shown as seasonal averages (right side, upper corner) and time-series of annual disequilibria (right side, lower corner). Blue line: North Sea, red line: Norwegian coast, yellow line: Barents Sea, purple line: Baltic Sea

The seasonal cycle of ΔfCO_2 follows a ~~mainly~~ biologically driven pattern with higher values in the winter and lower values from April to August. The seasonal cycle is largest in the Baltic and smallest in the Barents Sea.

The ~~sea-air~~ air-sea CO_2 fluxes and their trends (Figure 13) show that most regions are a net and increasing sink for CO_2. The only ~~source net~~ net source regions are the southern North Sea and the Baltic Sea. The two different regimes in the North Sea with the southern, nonstratified part being a source and the northern temporarily stratified part a sink for CO_2, ~~are well~~ have been described in the literature ~~(Thomas et al., 2004).~~ before (Thomas et al., 2004), but the gradient between them as represented here, may be a too sharp (Section 3.1). However, there is a large interannual variability in the fCO_2 disequilibrium (Omar et al., 2010) and studies based on different years find conflicting results regarding the direction of the flux (Kitidis et al., 2019; Schiettecatte et al., 2007; Thomas et al., 2004). This large interannual variability was also present in our maps. During some years, larger parts of the North Sea were a net source, while during other years also the southern North Sea acted as net sink (not shown).

The seasonal variations in the air-sea flux are driven by a combination of the changes in the disequilibrium, the wind strength, and the ice cover. As there is less wind during summer, when the disequilibrium is large, but a smaller disequilibrium during winter, when the wind strength is high, the seasonal variability in the flux is often less clear than that ~~of e.g. in~~ the disequilibrium. This can be seen in the Barents Sea and Norwegian Coast. Yasunaka et al. (2018) found the seasonal and interannual variation in the Barents Sea and the Norwegian Sea mostly corresponded to the wind speed and the sea ice concentration. ~~In contrast to that we~~ We see the strongest dependence on the air-sea disequilibrium~~. However, even though we don't find the same seasonality, considering the error margin and the small amplitude of the seasonality~~, however (not shown). This indicates that the seasonal and interannual variability in our fCO_2 maps is larger than in the maps generated by Yasunaka et al. (2018) . Still, our average fluxes fit well with those reported by Yasunaka et al. (2018) of -8 to -12 mmol m^{-2} d^{-1} (Barents Sea) and -4 to -8 mmol m^{-2} d^{-1} (Norwegian Coast). In the North Sea there is almost no net flux during winter, as the surface ocean is more or less in equilibrium with the atmosphere. In the Baltic Sea, ~~we can see~~ there are high fluxes into the atmosphere during winter as here a large oversaturation coincides with ~~high wind strengths~~strong winds. This is also why the Baltic Sea is a net source ~~regions~~region. Although Parard et al. (2017) did find slightly smaller seasonal fluxes (+15 mmol m^{-2} d^{-1} during winter and -8 mmol m^{-2} d^{-1} during summer), the annual air-sea CO_2 fluxes are in good agreement (0 to +4 mmol m^{-2} d^{-1} between 1998 and 2011).

The uncertainty in the calculated fluxes is a result of the uncertainties in the fCO_2 observations, ΔfCO_2 maps, the gas exchange parameterization and the wind product. The uncertainty of the ΔfCO_2 is mostly driven by the uncertainty of the MLR, resulting in an error between 12 μatm and 39 μatm, according to the RMSE values of MLR1 for the different regions (Table 5). A number of studies addresses ~~on~~ the uncertainty of gas exchange parameterizations and the wind products (Couldrey et al., 2016; Gregg et al., 2014; Ho and Wanninkhof, 2016). For this study, we apply an uncertainty of the gas transfer velocity of 20% (Wanninkhof, 2014). This will result in an uncertainty of the air-sea flux of about 2 mmol C d^{-1} m^{-2}. It has to be kept in mind, that the absolute uncertainty in k increases with increasing wind speed, but that the uncertainty in the wind speed has largest influence in summer when also the disequilibrium is large. In contrast~~to that~~ , the uncertainty in ΔfCO_2 will cause larger errors in winter, when the wind speeds are high.

There is an ongoing discussion, how and to which extent the dominant climate mode in the North Atlantic, the North Atlantic Oscillation (NAO) is driving the variability in the CO_2 fluxes (Salt et al., 2013; Tjiputra et al., 2012; Watson et al., 2009). Even though some features in the time series seem to coincide with very extreme states of the NAO, such as a very large disequilibrium along the Norwegian Coast in 2010, we could not find any significant correlation between the CO_2 fluxes and the NAO index.

5 Conclusions

The MLR approach presented in this work is a relatively easy and straight forward method to produce monthly fCO_2 maps with a high spatial resolution in coastal ~~regions. Using~~ seas, and the use of available open ocean maps ~~did improve~~ improved the coastal maps significantly. The maps reproduce nicely the main spatial and temporal patterns that ~~can also be found~~ present

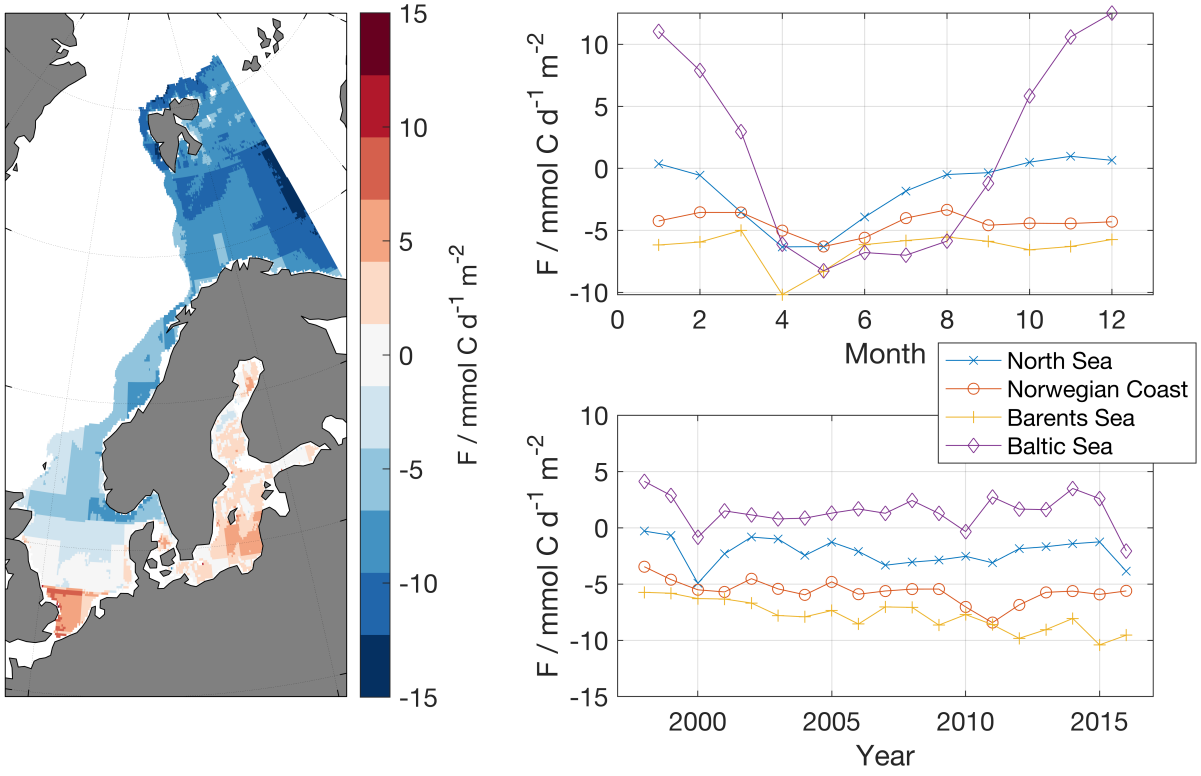

Figure 13. The average air-sea CO_2 flux over the period 1998-2016 (left hand panel, red colors indicate sink regions, while blue colors indicate source regions). For every region average fluxes are show as seasonal averages (right side, upper corner) and timeseries of annual fluxes (right side, lower corner).

in observations in the different regions for both fCO_2 and pH. The surface seawater fCO_2 trends were mostly lower than the atmospheric trends and also lower than the trends found in the open North Atlantic. ~~We did find~~ Results show that the northern European shelf ~~to be~~ is an increasing net sink for CO_2. Only the Baltic Sea is a net source region. This method clearly has the potential to be extended to a larger region. However, it should be handled with care in regions with only a small number of observations as the MLR can lead to unrealistic values.

Longterm observations with a high temporal resolution are extremely important for developing maps such as presented here. While a decent spatial coverage exists for the open North Atlantic, most coastal regions are still undersampled~~. This is in particular the case for higher latitudes and in the Arctic~~, in particular relative to their high variability in time and space. To further understand and interpret the trends ~~on~~ in fCO_2 and pH it is necessary to increase our knowledge and understanding of the interaction ~~of~~ between primary production, respiration in the water column and the sediments, mixing and gas exchange and their influence on the carbon cycle.

Besides an increased amount of insitu observations, also improved, higher resolution driver data hold the potential to enable a better representation of spatial gradients. Including not only satellite derived chlorophyll data, but also CDOM, can also lead to an improved performance of the regressions, especially in regions with a high load of terrestrial dissolved organic carbon.

While MLR derived sea surface ~~provides~~ fCO_2 maps provide a coherent picture of the entire region, they have clear limitations and should be interpreted with caution in regions with few or none observations. Both, for producing high quality maps, as well for their validation a large number of observations is essential.Also, observations of a second parameter of the carbon system would be beneficial for deriving pH maps~~. This will help ;~~ to reduce and quantify the error introduced by estimating alkalinity from salinity. In addition to that, our work neglects the areas closest to land due to unavailability of CO_2 data and reanalysis products in those areas. For adding their contribution to the flux estimates, new platforms specialized on measurements directly at the land-ocean interface need to be developed.

Data availability. The dataset is available under: https://doi.org/10.18160/939X-PMHU.

Appendix A: Trend in surface ocean fCO_2 observations

Competing interests. The authors declare no competing interests.

Acknowledgements. First of all, we want to thank everyone involved in the collection and quality control of surface ocean CO_2 data. The Surface Ocean CO_2 Atlas (SOCAT) is an international effort, endorsed by the International Ocean Carbon Coordination Project (IOCCP), the Surface Ocean Lower Atmosphere Study (SOLAS) and the Integrated Marine Biosphere Research (IMBeR) program, to deliver a uniformly quality-controlled surface ocean CO_2 database. The many researchers and funding agencies responsible for the collection of data and quality control are thanked for their contributions to SOCAT. We used NCEP Reanalysis 2 data provided by the NOAA/OAR/ESRL PSD, Boulder, Colorado, USA, from their web site at https://www.esrl.noaa.gov/psd/. This study has been conducted using E.U. Copernicus Marine Service Information. This ~~work~~ research was funded by the ~~project ICOS Norway (~~Research Council of Norway ~~,~~ projects ICOS-Norway (Grant 245927) ~~. This project has received funding from the~~ and Nansen Legacy (Grant 276730); the VERIFY project (European Union's Horizon 2020 research and innovation program ~~under~~ grant agreement No ~~776810. This work was supported by BONUS INTEGRAL, receiving funding from BONUS (Art 185)by the EU and the contributing national funding agencies, Grant No. 03F0773A of the German Ministry for Education and Research.~~ 776810); and BONUS Integral.

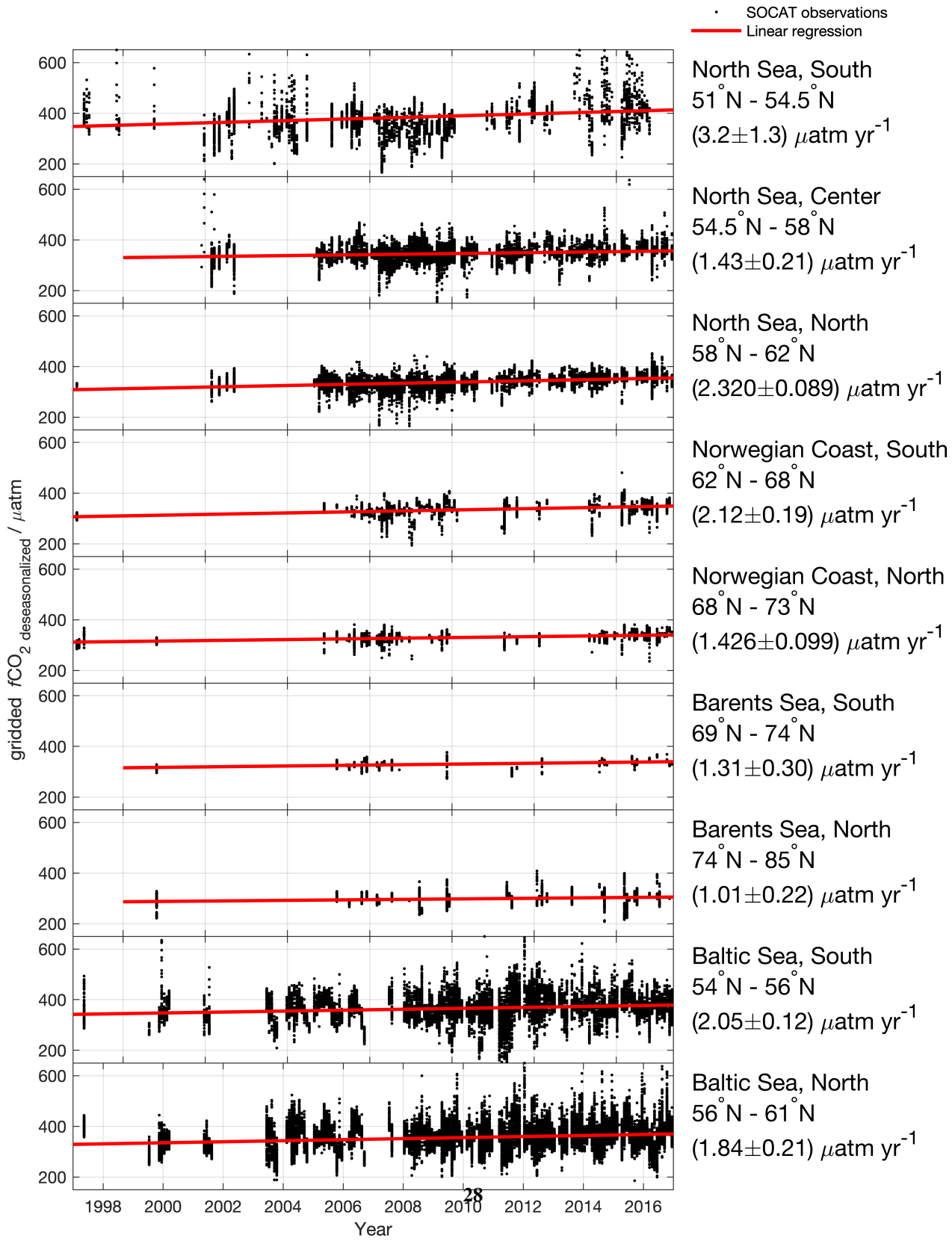
SOCAT observations
Linear regression
North Sea, South
51°N - 54.5°N
(3.2±1.3) μatm yr-1
North Sea, Center
54.5°N - 58°N
(1.43±0.21) μatm yr-1
North Sea, North
58°N - 62°N
(2.320±0.089) μatm yr-1
Norwegian Coast, South
62°N - 68°N
(2.12±0.19) μatm yr-1
Norwegian Coast, North
68°N - 73°N
(1.426±0.099) μatm yr-1
Barents Sea, South
69°N - 74°N
(1.31±0.30) μatm yr-1
Barents Sea, North
74°N - 85°N
(1.01±0.22) μatm yr-1
Baltic Sea, South
54°N - 56°N
(2.05±0.12) μatm yr-1
Baltic Sea, North
56°N - 61°N
(1.84±0.21) μatm yr-1
gridded fCO2 deseasonalized / μatm
200
400
600
1998
2000
2002
2004
2006
2008
2010
2012
2014
2016
Year

References

Bakker, D. C. E., Pfeil, B., Landa, C. S., Metzl, N., O'Brien, K. M., Olsen, A., Smith, K., Cosca, C., Harasawa, S., Jones, S. D., Nakaoka, S.-i., Nojiri, Y., Schuster, U., Steinhoff, T., Sweeney, C., Takahashi, T., Tilbrook, B., Wada, C., Wanninkhof, R., Alin, S. R., Balestrini, C. F., Barbero, L., Bates, N. R., Bianchi, A. A., Bonou, F., Boutin, J., Bozec, Y., Burger, E. F., Cai, W.-J., Castle, R. D., Chen, L., Chierici, M., Currie, K., Evans, W., Featherstone, C., Feely, R. A., Fransson, A., Goyet, C., Greenwood, N., Gregor, L., Hankin, S., Hardman-Mountford, N. J., Harlay, J., Hauck, J., Hoppema, M., Humphreys, M. P., Hunt, C. W., Huss, B., Ibánhez, J. S. P., Johannessen, T., Keeling, R., Kitidis, V., Körtzinger, A., Kozyr, A., Krasakopoulou, E., Kuwata, A., Landschützer, P., Lauvset, S. K., Lefèvre, N., Monaco, C. L., Manke, A., Mathis, J. T., Merlivat, L., Millero, F. J., Monteiro, P. M. S., Munro, D. R., Murata, A., Newberger, T., Omar, A. M., Ono, T., Paterson, K., Pearce, D., Pierrot, D., Robbins, L. L., Saito, S., Salisbury, J., Schlitzer, R., Schneider, B., Schweitzer, R., Sieger, R., Skjelvan, I., Sullivan, K. F., Sutherland, S. C., Sutton, A. J., Tadokoro, K., Telszewski, M., Tuma, M., Heuven, S. M. A. C. v., Vandemark, D., Ward, B., Watson, A. J., and Xu, S.: A multi-decade record of high-quality fCO_2 data in version 3 of the Surface Ocean CO_2 Atlas (SOCAT), Earth System Science Data, 8, 383–413, https://doi.org/https://doi.org/10.5194/essd-8-383-2016, https://www.earth-syst-sci-data.net/8/383/2016/, 2016.

Bauer, J. E., Cai, W.-J., Raymond, P. A., Bianchi, T. S., Hopkinson, C. S., and Regnier, P. A. G.: The changing carbon cycle of the coastal ocean, Nature, 504, 61–70, https://doi.org/10.1038/nature12857, https://www.nature.com/articles/nature12857, 2013.

Blanton, J. O.: Circulation processes along oceanic margins in relation to material fluxes, in: Ocean Margin Processes in Global Change, pp. 145–63, Wiley, New York, 1991.

Borges, A. V. and Gypens, N.: Carbonate chemistry in the coastal zone responds more strongly to eutrophication than ocean acidification, Limnology and Oceanography, 55, 346–353, https://doi.org/10.4319/lo.2010.55.1.0346, https://aslopubs.onlinelibrary.wiley.com/doi/abs/10.4319/lo.2010.55.1.0346, _eprint: https://aslopubs.onlinelibrary.wiley.com/doi/pdf/10.4319/lo.2010.55.1.0346, 2010.

Bourgeois, T., Orr, J. C., Resplandy, L., Terhaar, J., Ethé, C., Gehlen, M., and Bopp, L.: Coastal-ocean uptake of anthropogenic carbon, Biogeosciences, 13, 4167–4185, https://doi.org/https://doi.org/10.5194/bg-13-4167-2016, https://www.biogeosciences.net/13/4167/2016/, 2016.

Bricheno, L. M., Wolf, J. M., and Brown, J. M.: Impacts of high resolution model downscaling in coastal regions, Continental Shelf Research, 87, 7–16, https://doi.org/10.1016/j.csr.2013.11.007, http://www.sciencedirect.com/science/article/pii/S0278434313003725, 2014.

Cai, W.-J., Hu, X., Huang, W.-J., Murrell, M. C., Lehrter, J. C., Lohrenz, S. E., Chou, W.-C., Zhai, W., Hollibaugh, J. T., Wang, Y., Zhao, P., Guo, X., Gundersen, K., Dai, M., and Gong, G.-C.: Acidification of subsurface coastal waters enhanced by eutrophication, Nature Geosci, 4, 766–770, https://doi.org/10.1038/ngeo1297, https://www.nature.com/articles/ngeo1297, number: 11 Publisher: Nature Publishing Group, 2011.

Cavalieri, D. J., Parkinson, C. L., Gloersen, P., and Zwally, H. J.: Sea Ice Concentrations from Nimbus-7 SMMR and DMSP SSM/I-SSMIS Passive Microwave Data, Version 1, Monthly, doi:https://doi.org/10.5067/8GQ8LZQVL0VL, 1996.

Center, N. G. D.: 2-minute Gridded Global Relief Data (ETOPO2) v2, NOAA, https://doi.org/doi:10.7289/V5J1012Q, 2006.

"Cooperative Global Atmospheric Data Integration Project": Multi-laboratory compilation of atmospheric carbon dioxide data for the period 1968-2014, obspack_co2_1_GLOBALVIEWplus_v1.0_2015-07-30, https://doi.org/10.15138/G3RP42, published: NOAA Earth System Research Laboratory, Global Monitoring Division, 2015.

Couldrey, M. P., Oliver, K. I. C., Yool, A., Halloran, P. R., and Achterberg, E. P.: On which timescales do gas transfer velocities control North Atlantic CO2 flux variability?, Global Biogeochemical Cycles, 30, 787–802, https://doi.org/10.1002/2015GB005267, https://agupubs.onlinelibrary.wiley.com/doi/abs/10.1002/2015GB005267, 2016.

Desmit, X., Nohe, A., Borges, A. V., Prins, T., Cauwer, K. D., Lagring, R., Zande, D. V. d., and Sabbe, K.: Changes in chlorophyll concentration and phenology in the North Sea in relation to de-eutrophication and sea surface warming, Limnology and Oceanography, 65, 828–847, https://doi.org/10.1002/lno.11351, https://aslopubs.onlinelibrary.wiley.com/doi/abs/10.1002/lno.11351, _eprint: https://aslopubs.onlinelibrary.wiley.com/doi/pdf/10.1002/lno.11351, 2020.

Dickson, A. and Millero, F.: A comparison of the equilibrium constants for the dissociation of carbonic acid in seawater media, Deep-Sea Res. Pt I, 34, 1733 – 1743, https://doi.org/10.1016/0198-0149(87)90021-5, 1987.

Dickson, A. G.: Standard potential of the reaction: AgCl(s) + 12H2(g) = Ag(s) + HCl(aq), and and the standard acidity constant of the ion HSO4 in synthetic sea water from 273.15 to 318.15 K, The Journal of Chemical Thermodynamics, 22, 113–127, https://doi.org/10.1016/0021-9614(90)90074-Z, http://www.sciencedirect.com/science/article/pii/002196149090074Z, 1990.

Fay, A. R. and McKinley, G. A.: Correlations of surface ocean pCO2 to satellite chlorophyll on monthly to interannual timescales, Global Biogeochemical Cycles, 31, 436–455, https://doi.org/10.1002/2016GB005563, https://agupubs.onlinelibrary.wiley.com/doi/abs/10.1002/2016GB005563, 2017.

Fröb, F., Olsen, A., Becker, M., Chafik, L., Johannessen, T., Reverdin, G., and Omar, A.: Wintertime fCO2 Variability in the Subpolar North Atlantic Since 2004, Geophysical Research Letters, 46, 1580–1590, https://doi.org/10.1029/2018GL080554, https://agupubs.onlinelibrary.wiley.com/doi/abs/10.1029/2018GL080554, 2019.

Gregg, W. W., Casey, N. W., and Rousseaux, C. S.: Sensitivity of simulated global ocean carbon flux estimates to forcing by reanalysis products, Ocean Modelling, 80, 24–35, https://doi.org/10.1016/j.ocemod.2014.05.002, http://www.sciencedirect.com/science/article/pii/S1463500314000651, 2014.

Griffiths, J. R., Kadin, M., Nascimento, F. J. A., Tamelander, T., Törnroos, A., Bonaglia, S., Bonsdorff, E., Brüchert, V., Gårdmark, A., Järnström, M., Kotta, J., Lindegren, M., Nordström, M. C., Norkko, A., Olsson, J., Weigel, B., Žydelis, R., Blenckner, T., Niiranen, S., and Winder, M.: The importance of benthic–pelagic coupling for marine ecosystem functioning in a changing world, Global Change Biology, 23, 2179–2196, https://doi.org/10.1111/gcb.13642, https://onlinelibrary.wiley.com/doi/abs/10.1111/gcb.13642, 2017.

Gruber, N., Clement, D., Carter, B. R., Feely, R. A., Heuven, S. v., Hoppema, M., Ishii, M., Key, R. M., Kozyr, A., Lauvset, S. K., Monaco, C. L., Mathis, J. T., Murata, A., Olsen, A., Perez, F. F., Sabine, C. L., Tanhua, T., and Wanninkhof, R.: The oceanic sink for anthropogenic CO2 from 1994 to 2007, Science, 363, 1193–1199, https://doi.org/10.1126/science.aau5153, http://science.sciencemag.org/content/363/6432/1193, 2019.

Ho, D. T. and Wanninkhof, R.: Air–sea gas exchange in the North Atlantic: 3He/SF6 experiment during GasEx-98, Tellus B: Chemical and Physical Meteorology, 68, 30 198, https://doi.org/10.3402/tellusb.v68.30198, https://doi.org/10.3402/tellusb.v68.30198, 2016.

Jones, S. D., Quéré, C. L., Rödenbeck, C., Manning, A. C., and Olsen, A.: A statistical gap-filling method to interpolate global monthly surface ocean carbon dioxide data, Journal of Advances in Modeling Earth Systems, 7, 1554–1575, https://doi.org/10.1002/2014MS000416, https://agupubs.onlinelibrary.wiley.com/doi/abs/10.1002/2014MS000416, 2015.

Kanamitsu, M., Ebisuzaki, W., Woollen, J., Yang, S.-K., Hnilo, J. J., Fiorino, M., and Potter, G. L.: NCEP–DOE AMIP-II Reanalysis (R-2), Bull. Amer. Meteor. Soc., 83, 1631–1644, https://doi.org/10.1175/BAMS-83-11-1631, https://journals.ametsoc.org/doi/abs/10.1175/BAMS-83-11-1631, 2002.

Kitidis, V., Shutler, J. D., Ashton, I., Warren, M., Brown, I., Findlay, H., Hartman, S. E., Sanders, R., Humphreys, M., Kivimäe, C., Greenwood, N., Hull, T., Pearce, D., McGrath, T., Stewart, B. M., Walsham, P., McGovern, E., Bozec, Y., Gac, J.-P., van Heuven, S. M. A. C., Hoppema, M., Schuster, U., Johannessen, T., Omar, A., Lauvset, S. K., Skjelvan, I., Olsen, A., Steinhoff, T., Körtzinger, A., Becker, M., Lefevre, N., Diverrès, D., Gkritzalis, T., Cattrijsse, A., Petersen, W., Voynova, Y. G., Chapron, B., Grouazel, A., Land, P. E., Sharples, J., and Nightingale, P. D.: Winter weather controls net influx of atmospheric CO 2 on the north-west European shelf, Scientific Reports, 9, 20 153, https://doi.org/10.1038/s41598-019-56363-5, https://www.nature.com/articles/s41598-019-56363-5, number: 1 Publisher: Nature Publishing Group, 2019.

Landschützer, P., Gruber, N., Bakker, D. C. E., Schuster, U., Nakaoka, S., Payne, M. R., Sasse, T. P., and Zeng, J.: A neural network-based estimate of the seasonal to inter-annual variability of the Atlantic Ocean carbon sink, Biogeosciences, 10, 7793–7815, https://doi.org/10.5194/bg-10-7793-2013, 2013.

Landschützer, P., Gruber, N., Bakker, D. C. E., and Schuster, U.: Recent variability of the global ocean carbon sink, Global Biogeochem. Cycles, 28, 927–949, https://doi.org/10.1002/2014GB004853, 2014.

Landschützer, P., Gruber, N., and Bakker, D. C. E.: Decadal variations and trends of the global ocean carbon sink, Global Biogeochemical Cycles, 30, 1396–1417, https://doi.org/10.1002/2015GB005359, https://agupubs.onlinelibrary.wiley.com/doi/abs/10.1002/2015GB005359, 2016.

Landschützer, P., Gruber, N., and Bakker, D. C. E.: An updated observation-based global monthly gridded sea surface pCO2 and air-sea CO2 flux product from 1982 through 2015 and its monthly climatology (NCEI Accession 0160558). Version 2.2., 2017.

Landschützer, P., Gruber, N., Bakker, D. C. E., Stemmler, I., and Six, K. D.: Strengthening seasonal marine CO 2 variations due to increasing atmospheric CO 2, Nature Climate Change, 8, 146, https://doi.org/10.1038/s41558-017-0057-x, https://www.nature.com/articles/s41558-017-0057-x, 2018.

Landschützer, P., Ilyina, T., and Lovenduski, N. S.: Detecting Regional Modes of Variability in Observation-Based Surface Ocean pCO2, Geophysical Research Letters, 0, https://doi.org/10.1029/2018GL081756, https://agupubs.onlinelibrary.wiley.com/doi/abs/10.1029/2018GL081756, 2019.

Landschützer, P., Laruelle, G. G., Roobaert, A., and Regnier, P.: A uniform pCO_2 climatology combining open and coastal oceans, Earth System Science Data Discussions, pp. 1–30, https://doi.org/https://doi.org/10.5194/essd-2020-90, https://essd.copernicus.org/preprints/essd-2020-90/, publisher: Copernicus GmbH, 2020.

Laruelle, G. G., Dürr, H. H., Slomp, C. P., and Borges, A. V.: Evaluation of sinks and sources of CO2 in the global coastal ocean using a spatially-explicit typology of estuaries and continental shelves, Geophysical Research Letters, 37, https://doi.org/10.1029/2010GL043691, https://agupubs.onlinelibrary.wiley.com/doi/abs/10.1029/2010GL043691, 2010.

Laruelle, G. G., Dürr, H. H., Lauerwald, R., Hartmann, J., Slomp, C. P., Goossens, N., and Regnier, P. a. G.: Global multi-scale segmentation of continental and coastal waters from the watersheds to the continental margins, Hydrology and Earth System Sciences, 17, 2029–2051, https://doi.org/https://doi.org/10.5194/hess-17-2029-2013, https://www.hydrol-earth-syst-sci.net/17/2029/2013/, 2013.

Laruelle, G. G., Landschützer, P., Gruber, N., Tison, J.-L., Delille, B., and Regnier, P.: Global high-resolution monthly pCO_2 climatology for the coastal ocean derived from neural network interpolation, Biogeosciences, 14, 4545–4561, https://doi.org/https://doi.org/10.5194/bg-14-4545-2017, https://www.biogeosciences.net/14/4545/2017/, 2017.

Laruelle, G. G., Cai, W.-J., Hu, X., Gruber, N., Mackenzie, F. T., and Regnier, P.: Continental shelves as a variable but increasing global sink for atmospheric carbon dioxide, Nature Communications, 9, 454, https://doi.org/10.1038/s41467-017-02738-z, https://www.nature.com/articles/s41467-017-02738-z, 2018.

Lauvset, S. K. and Gruber, N.: Long-term trends in surface ocean pH in the North Atlantic, Marine Chemistry, 162, 71–76, https://doi.org/10.1016/j.marchem.2014.03.009, https://www.sciencedirect.com/science/article/pii/S0304420314000607, 2014.

Lauvset, S. K., Gruber, N., Landschützer, P., Olsen, A., and Tjiputra, J.: Trends and drivers in global surface ocean pH over the past 3 decades, Biogeosciences, 12, 1285–1298, https://doi.org/https://doi.org/10.5194/bg-12-1285-2015, https://www.biogeosciences.net/12/1285/2015/, 2015.

Lima, F. P. and Wethey, D. S.: Three decades of high-resolution coastal sea surface temperatures reveal more than warming, Nat Commun, 3, 1–13, https://doi.org/10.1038/ncomms1713, https://www.nature.com/articles/ncomms1713, 2012.

Lind, S., Ingvaldsen, R. B., and Furevik, T.: Arctic warming hotspot in the northern Barents Sea linked to declining sea-ice import, Nature Clim Change, 8, 634–639, https://doi.org/10.1038/s41558-018-0205-y, https://www.nature.com/articles/s41558-018-0205-y, 2018.

Locarnini, R., Mishonov, A., Baranova, O., Boyer, T., Zweng, M., GarciA, H., Reagan, J., Seidov, D., Weathers, K., Paver, C., and Smoylar, I.: World Ocean Atlas 2018, Volume 1: Temperature, A. Mishonov Technical Ed., 2018.

Loose, B., McGillis, W. R., Schlosser, P., Perovich, D., and Takahashi, T.: Effects of freezing, growth, and ice cover on gas transport processes in laboratory seawater experiments, Geophysical Research Letters, 36, https://doi.org/10.1029/2008GL036318, https://agupubs.onlinelibrary.wiley.com/doi/abs/10.1029/2008GL036318, 2009.

Mehrbach, C., Culberson, C., Hawley, J., and Pytkowicz, R.: Measurement of the apparent dissociation constants of carbonic acid in seawater at atmospheric pressure, Limnol. Oceanogr., 18, 897–907, 1973.

Meyer, M., Pätsch, J., Geyer, B., and Thomas, H.: Revisiting the Estimate of the North Sea Air-Sea Flux of CO2 in 2001/2002: The Dominant Role of Different Wind Data Products, Journal of Geophysical Research: Biogeosciences, 123, 1511–1525, https://doi.org/10.1029/2017JG004281, https://agupubs.onlinelibrary.wiley.com/doi/abs/10.1029/2017JG004281, 2018.

Müller, J. D., Schneider, B., and Rehder, G.: Long-term alkalinity trends in the Baltic Sea and their implications for CO2-induced acidification, Limnology and Oceanography, 61, 1984–2002, https://doi.org/10.1002/lno.10349, https://aslopubs.onlinelibrary.wiley.com/doi/abs/10.1002/lno.10349, 2016.

Naegler, T.: Reconciliation of excess 14C-constrained global CO2 piston velocity estimates, Tellus B: Chemical and Physical Meteorology, 61, 372–384, https://doi.org/10.1111/j.1600-0889.2008.00408.x, https://doi.org/10.1111/j.1600-0889.2008.00408.x, 2009.

Nondal, G., Bellerby, R. G. J., Oldenc, A., Johannessena, T., and Olafssond, J.: Optimal evaluation of the surface ocean CO2 system in the northern North Atlantic using data from voluntary observing ships, Limnol. Oceanogr., 7, 109–118, 2009.

Omar, A. M., Olsen, A., Johannessen, T., Hoppema, M., Thomas, H., and Borges, A. V.: Spatiotemporal variations of f CO2 in the North Sea, Ocean Sci., p. 13, 2010.

Omar, A. M., Thomas, H., Olsen, A., Becker, M., Skjelvan, I., and Reverdin, G.: Trend of ocean acidification and pCO2 in the northern North Sea, 2004-2015, Journal of Geophysical Research - Biogeosciences, 2019.

Oziel, L., Neukermans, G., Ardyna, M., Lancelot, C., Tison, J.-L., Wassmann, P., Sirven, J., Ruiz-Pino, D., and Gascard, J.-C.: Role for Atlantic inflows and sea ice loss on shifting phytoplankton blooms in the Barents Sea, Journal of Geophysical Research: Oceans, pp. 5121–5139, https://doi.org/10.1002/2016JC012582@10.1002/(ISSN)2169-9291.ARCTICJOINT, https://agupubs.onlinelibrary.wiley.com/doi/abs/10.1002/2016JC012582%4010.1002/%28ISSN%292169-9291.ARCTICJOINT, 2016.

Parard, G., Charantonis, A. A., and Rutgersson, A.: Using satellite data to estimate partial pressure of CO_2 in the Baltic Sea: PARTIAL PRESSURE OF CO_2 VARIABILITY, Journal of Geophysical Research: Biogeosciences, 121, 1002–1015, https://doi.org/10.1002/2015JG003064, http://doi.wiley.com/10.1002/2015JG003064, 2016.

Parard, G., Rutgersson, A., Raj Parampil, S., and Charantonis, A. A.: The potential of using remote sensing data to estimate air–sea CO₂ exchange in the Baltic Sea, Earth System Dynamics, 8, 1093–1106, https://doi.org/10.5194/esd-8-1093-2017, https://www.earth-syst-dynam.net/8/1093/2017/, 2017.

Pierrot, D., Neill, C., Sullivan, K., Castle, R., Wanninkhof, R., Lüger, H., Johannessen, T., Olsen, A., Feely, R. A., and Cosca, C. E.: Recommendations for autonomous underway $p\mathrmCO_2$ measuring systems and data-reduction routines, Surface Ocean CO2 Variability and Vulnerabilities, 56, 512–522, https://doi.org/10.1016/j.dsr2.2008.12.005, 2009.

Roobaert, A., Laruelle, G. G., Landschützer, P., and Regnier, P.: Uncertainty in the global oceanic CO_2 uptake induced by wind forcing: quantification and spatial analysis, Biogeosciences, 15, 1701–1720, https://doi.org/https://doi.org/10.5194/bg-15-1701-2018, https://www.biogeosciences.net/15/1701/2018/, 2018.

Rödenbeck, C., Keeling, R. F., Bakker, D. C. E., Metzl, N., Olsen, A., Sabine, C., and Heimann, M.: Global surface-ocean pCO2 and sea–air CO2 flux variability from an observation-driven ocean mixed-layer scheme, Ocean Sci., 9, 193–216, https://doi.org/10.5194/os-9-193-2013, https://www.ocean-sci.net/9/193/2013/, 2013.

Rödenbeck, C., Bakker, D. C. E., Metzl, N., Olsen, A., Sabine, C., Cassar, N., Reum, F., Keeling, R. F., and Heimann, M.: Interannual sea–air CO_2 flux variability from an observation-driven ocean mixed-layer scheme, Biogeosciences, 11, 4599–4613, https://doi.org/https://doi.org/10.5194/bg-11-4599-2014, https://www.biogeosciences.net/11/4599/2014/bg-11-4599-2014.html, 2014.

Rödenbeck, C., Bakker, D. C. E., Gruber, N., Iida, Y., Jacobson, A. R., Jones, S., Landschützer, P., Metzl, N., Nakaoka, S., Olsen, A., Park, G.-H., Peylin, P., Rodgers, K. B., Sasse, T. P., Schuster, U., Shutler, J. D., Valsala, V., Wanninkhof, R., and Zeng, J.: Data-based estimates of the ocean carbon sink variability – first results of the Surface Ocean pCO_2 Mapping intercomparison (SOCOM), Biogeosciences, 12, 7251–7278, https://doi.org/https://doi.org/10.5194/bg-12-7251-2015, https://www.biogeosciences.net/12/7251/2015/, 2015.

Salt, L. A., Thomas, H., Prowe, A. E. F., Borges, A. V., Bozec, Y., and Baar, H. J. W. d.: Variability of North Sea pH and CO2 in response to North Atlantic Oscillation forcing, Journal of Geophysical Research: Biogeosciences, 118, 1584–1592, https://doi.org/10.1002/2013JG002306, https://agupubs.onlinelibrary.wiley.com/doi/abs/10.1002/2013JG002306, 2013.

Schiettecatte, L. S., Thomas, H., Bozec, Y., and Borges, A. V.: High temporal coverage of carbon dioxide measurements in the Southern Bight of the North Sea, Marine Chemistry, 106, 161–173, https://doi.org/10.1016/j.marchem.2007.01.001, http://www.sciencedirect.com/science/article/pii/S0304420307000023, 2007.

Schneider, B. and Müller, J. D.: Biogeochemical Transformations in the Baltic Sea: Observations Through Carbon Dioxide Glasses, Springer Oceanography, Springer International Publishing, https://www.springer.com/gp/book/9783319616988, 2018.

Sharples, J., Ross, O. N., Scott, B. E., Greenstreet, S. P. R., and Fraser, H.: Inter-annual variability in the timing of stratification and the spring bloom in the North-western North Sea, Cont.Shelf Res., 26, 733–751, https://doi.org/10.1016/j.csr.2006.01.011, https://abdn.pure.elsevier.com/en/publications/inter-annual-variability-in-the-timing-of-stratification-and-the-, 2006.

Thomas, H., Bozec, Y., Elkalay, K., and Baar, H. J. W. d.: Enhanced Open Ocean Storage of CO2 from Shelf Sea Pumping, Science, 304, 1005–1008, https://doi.org/10.1126/science.1095491, https://science.sciencemag.org/content/304/5673/1005, 2004.

Thomas, H., Friederike Prowe, A. E., van Heuven, S., Bozec, Y., de Baar, H. J. W., Schiettecatte, L.-S., Suykens, K., Koné, M., Borges, A. V., Lima, I. D., and Doney, S. C.: Rapid decline of the CO2 buffering capacity in the North Sea and implications for the North Atlantic Ocean, Global Biogeochemical Cycles, 21, https://doi.org/10.1029/2006GB002825, https://agupubs.onlinelibrary.wiley.com/doi/full/10.1029/2006GB002825, 2007.

Tjiputra, J., Olsen, A., Assmann, K. M., Pfeil, B., and Heinze, C.: A model study of the seasonal and long-term North Atlantic surface pCO(2) variability, 1726-4170, https://doi.org/10.5194/bg-9-907-2012, https://bora.uib.no/handle/1956/17939, accepted: 2018-08-01T08:05:48Z Publisher: Copernicus Publications, 2012.

Uppström, L. R.: The boron/chlorinity ratio of deep-sea water from the Pacific Ocean, Deep Sea Research and Oceanographic Abstracts, 21, 161–162, https://doi.org/10.1016/0011-7471(74)90074-6, http://www.sciencedirect.com/science/article/pii/0011747174900746, 1974.

van Heuven, S., Pierrot, D., Lewis, E., and Wallace, D.: {MATLAB} Program Developed for {CO}$_2$ System Calculations. {ORNL/CDIAC}-105b., 2009.

Wanninkhof, R.: Relationship between wind speed and gas exchange over the ocean revisited: Gas exchange and wind speed over the ocean, Limnology and Oceanography: Methods, 12, 351–362, https://doi.org/10.4319/lom.2014.12.351, http://doi.wiley.com/10.4319/lom.2014.12.351, 2014.

Watson, A. J., Schuster, U., Bakker, D. C. E., Bates, N. R., Corbiere, A., Gonzalez-Davila, M., Friedrich, T., Hauck, J., Heinze, C., Johannessen, T., Kortzinger, A., Metzl, N., Olafsson, J., Olsen, A., Oschlies, A., Padin, X. A., Pfeil, B., Santana-Casiano, J. M., Steinhoff, T., Telszewski, M., Rios, A. F., Wallace, D. W. R., and Wanninkhof, R.: Tracking the Variable North Atlantic Sink for Atmospheric CO2, Science, 326, 1391–1393, 2009.

Weiss, R. F.: Carbon dioxide in water and seawater: The solubility of a non-ideal gas, Mar. Chem., 2, 203–215, 1974.

Wesslander, K., Omstedt, A., and Schneider, B.: Inter-annual and seasonal variations in the air–sea CO2 balance in the central Baltic Sea and the Kattegat, Continental Shelf Research, 30, 1511–1521, http://www.academia.edu/16389763/Inter-annual_and_seasonal_variations_in_the_air_sea_CO2_balance_in_the_central_Baltic_Sea_and_the_Kattegat, 2010.

Wollast, R.: Evaluation and comparison of the global carbon cycle in the coastal zone and in the open ocean, in: The Sea, edited by Brink, K. H. and Robinson, A. R., pp. 213–252, John Wiley & Sons, New York, 1998.

Yasunaka, S., Siswanto, E., Olsen, A., Hoppema, M., Watanabe, E., Fransson, A., Chierici, M., Murata, A., Lauvset, S. K., Wanninkhof, R., Takahashi, T., Kosugi, N., Omar, A. M., Heuven, S. v., and Mathis, J. T.: Arctic Ocean CO_2 uptake: an improved multiyear estimate of the air–sea CO_2 flux incorporating chlorophyll *a* concentrations, Biogeosciences, 15, 1643–1661, https://doi.org/https://doi.org/10.5194/bg-15-1643-2018, https://www.biogeosciences.net/15/1643/2018/, 2018.